SEASONAL ECOLOGICAL ASSESSMENT IN THE UPPER GUADALUPE ESTUARY

FINAL REPORT

Prepared for

Texas Water Development Board

Contract #2300012700

Prepared by

Kyle T. Sullivan

Christa R. Kunkel

Bradley M. Littrell

Edmund L. Oborny, Jr.

BIO-WEST, Inc.

1405 United Drive, Suite 111

San Marcos, Texas 78666

APRIL 2025

Pursuant to House Bill 1 as approved by the 87th Texas Legislature, this study report was funded for the purpose of studying environmental flow needs for Texas rivers and estuaries as part of the adaptive management phase of the Senate Bill 3 process for environmental flows established by the 80th Texas Legislature. The views and conclusions expressed herein are those of the author(s) and do not necessarily reflect the views of the Texas Water Development Board.

TABLE OF CONTENTS

LIST OF FIGURES

LIST OF TABLES

LIST OF ACRONYMS

BIO-WEST:	BIO-WEST, Inc.
ARU:	automated recording unit
%:	percent
°C:	degrees Celsius
AIC:	Akaike Information Criteria
BBEST:	Basin and Bay Area Expert Science Team
BIC:	Bayesian Information Criteria
cfs:	cubic feet per second
CI:	confidence interval
D:	dispersion
Delta:	Guadalupe River Delta
DO:	dissolved oxygen
ED:	estuarine-dependent
EM:	emergent marsh
ER:	estuarine-resident
FE:	fixed effect
FW:	freshwater
FWI:	freshwater inflow
GSA BBASC:	Guadalupe, San Antonio, Mission, and Aransas Rivers and Mission, Copano, Aransas and San Antonio Bays Basin and Bay Area Stakeholder Committee
ind/m^2:	individuals per square-meter
m, m^2:	meters, square-meters
ME:	marsh edge
MF:	mudflat
mg/L:	milligrams per liter
NMDS:	non-metric multidimensional scaling
NOAA:	National Oceanic and Atmospheric Administration
OW:	open water
PCA:	principal component analysis
ppt:	parts per thousand
Q10, Q50, Q90:	10th percentile, 50th percentile, 90th percentile
r:	correlation coefficient
R^2:	variation explained
RE:	random effect

RMSE:	root mean squared error
S1-S5:	Site 1-5
SB:	non-vegetated bay bottom
SB3:	Senate Bill 3
SL:	shoreline
TCEQ:	Texas Commission on Environmental Quality
TL:	tide-level
TWDB:	Texas Water Development Board
USDA:	U.S. Department of Agriculture
USGS:	U.S. Geological Survey
WL:	woodland
Workplan:	workplan for adaptive management
μS/cm:	micro siemens per centimeter

EXECUTIVE SUMMARY

Passage of Senate Bill 3 (SB3) by the 80th Texas Legislature in 2007 established a process to develop and implement environmental flow standards for each of the major rivers and estuaries in Texas. This process resulted in establishment of the Guadalupe, San Antonio, Mission, and Aransas Rivers, and Mission, Copano, Aransas, and San Antonio Bays Basin and Bay Area Stakeholders Committee (GSA BBASC) that, working with an expert science team, was charged with developing environmental flow recommendations for the specified basin and bay area. Ultimately, the process led to adoption of environmental flow standards for this area by the Texas Commission on Environmental Quality (TCEQ), which became effective on August 30, 2012.

As part of the process, the GSA BBASC also submitted a Work Plan for Adaptive Management (Workplan), which identified data gaps and prioritized additional research tasks for validation and refinement of environmental flow recommendations and standards. The Workplan identified life cycle, habitat, and salinity studies for key bay and estuary faunal species as a Tier 1 high-priority task. It also called for additional studies on distribution and abundance of marsh vegetation in relation to salinity and elevation in the Guadalupe Delta. This multi-year, Texas Water Development Board (TWDB) funded study effort described herein was conducted to supplement the available data on these priority research tasks. Specific objectives of the study were to initiate establishment of baseline conditions of marsh productivity for the upper Guadalupe Delta, evaluate the role of salinity and inundation relative to marsh vegetation community dynamics, and quantify aquatic organism species abundance and community composition within shallow habitats in relation to physical habitat and salinity.

To accomplish this, three sampling sites were first established within the Guadalupe River Delta (hereafter 'the Delta') along a longitudinal gradient from near the sources of freshwater inflow to near the tip of the Delta in close proximity to open bay areas. Initial surveys were conducted in 2019 to establish baseline conditions of the vegetation and faunal assemblages within the Delta. Continuation of seasonal monitoring was performed in 2021, which included the initiation of avian community surveys. In 2023 and 2024, the temporal extent of sampling was extended across all four seasons and two new sites were added for sampling.

To bracket the growing season, species composition and relative abundance, and biomass of the marsh vegetation community were quantified from multiple plots along fixed transects at each site in spring and fall. To establish a baseline of avian community composition, timed point counts were utilized to quantify species abundance, diversity, and describe differences in assemblage structure among sites and across seasons. To target seasons when key economically important faunal species are utilizing shallow estuarine areas, nekton sampling was conducted using throw-traps in spring, summer, fall, and winter. Fish, macrocrustaceans (i.e., shrimp and crabs), and mollusks were quantified from each throw-trap sample. Habitat (e.g., emergent and submergent vegetation composition and coverage) and water quality (e.g., salinity, water temperature) conditions were quantified to examine relationships between taxa occurrence/abundance and environmental variables. Descriptive, multivariate, and regression-based statistical methods were used to examine spatiotemporal patterns in community composition, species habitat associations, and biological productivity.

A diverse community of wetland and marsh plants were documented, with a distinct longitudinal gradient in species composition apparent across sites, following a pattern in long-term salinity conditions. Vegetation communities sampled in 2023 exhibited a gradient of freshwater-associated to saltwater-associated species assemblages similar to those reported in previous years. Areas closer to the freshwater influence of the Guadalupe River were characterized by emergent freshwater marsh plants and non-native species, with more saline sites adjacent to bays generally dominated by facultative halophytes (i.e., tolerant to a wide range of salinities). Expanded sampling areas in 2021 and 2023-2024 likely contributed to increased species overlap and diversity observed among Site 1-3. The addition of two new sites also provided a greater understanding of spatial patterns in vegetation communities across the Delta. Most significantly, the prevalence of Carolina Wolfberry at Site 5 indicated emergent marshes in this area provide food resources and habitat for the endangered Whooping Crane.

The avian community assessment demonstrated the high-level of diversity present within the Delta. This estuary provides a wide array of habitat types which support migratory and resident species from a variety of foraging guilds. Community composition was not dominated by any particular taxa, though four species represented about 40% of all individuals; Red-winged Blackbird (10.7%), Cattle Egret (10.1%), Brown Pelican (10.1%), and Boat-tailed Grackle (9.5%). Twenty-two species were ubiquitously observed across the Delta and each site contained a unique subset of taxa. Addition of Site 4 and 5 and a winter survey event helped to better characterize both the spatial and temporal variability of avian assemblage structure throughout the Delta. As reference above, detections of endangered Whooping Cranes at Site 5 may be related to the presence of Caroline Wolfberry in this area, which is a common Whooping Crane food source. Surveys failed to detect Eastern Black Rail, though recent observations of this cryptic species during 2021 surveys suggest it still occurs in the Delta. Species-specific survey techniques may be necessary to improve detectability of Eastern Black Rail and help to better understand their population. Lastly, neither listed species were detected by automated recorders, suggesting the need to select alternate or additional deployment locations in the future.

Assessments of nekton communities in the Delta generally aligned with past observations, but illustrated several novel findings. Spatiotemporal variation in nekton assemblage structure and among estuary use guilds were associated with both stationary (e.g., vegetation) and dynamic (e.g., salinity) habitat components. Most significantly, the mixed effects model used for this report was able to use freshwater inflow and tide characteristics to predict variation in nekton density with good accuracy. Results from the final model selected for inference indicated effects of 180-day high flow pulse frequency were linear, whereas effects of 90-day average tide level were nonlinear, further supporting that interactions between large scale environmental processes and biotic communities in estuaries are complex. The positive effect illustrated by 180-day high flow pulse frequency on nekton density demonstrated that increases in freshwater inflow can enhance biological productivity. In addition, the stronger effect size illustrated by tide level suggests maintaining hydrologic connectivity between the Delta and bay complexes is also important. In total, this supports that freshwater inflow and tidal regimes are both key determinants of biological productivity in the upper Guadalupe Estuary.

In summary, synthesis of all data collected in the Guadalupe River Delta over the entire study duration both supported results from previous analyses and provided new insights on potential mechanisms driving spatiotemporal patterns in diversity, assemblage structure, and productivity of biotic communities. High variability implicit with estuaries makes it difficult to accurately quantify the complexities of these systems. However, the additional data collected in 2023 and 2024 helped to enhance current knowledge on ecological processes dictating ecosystem function in the Delta. Further sampling effort could help to refine mechanistic relationships between inflows, tides, and ecological function. Future endeavors might benefit from sampling areas beyond emergent marsh habitats of the Delta and expanding into other major habitat units within secondary and primary bay complexes (e.g., seagrass beds, barrier islands, lagoons) to provide a more holistic assessment on the ecology of the Guadalupe Estuary.

1.0 INTRODUCTION

Estuarine ecosystems are particularly complex due to the interaction between freshwater and marine processes (Methven et al. 2001; Elliot and Hemingway 2002; Akin et al. 2003). Spatial configuration of estuaries generally includes river deltas that contain a variety of habitat types (e.g., tidal freshwater, salt marsh), secondary bays and lakes which rivers and streams flow into, and a primary bay directly connected to the sea (Montagna et al. 2011). Therefore, estuaries provide important spawning, nursery, feeding, and migration habitats for a wide array of species (Montagna et al. 2011; Cowan et al. 2012). Biotic communities generally consist of a combination of freshwater and euryhaline (i.e., adapted to a wide range of salinities) taxa. Composition and abundance of estuarine biota vary substantially across space and time, which depend on both the spatial configuration of major habitat units and spatiotemporal dynamics of physiochemical processes (Peterson 2003; Montagna et al. 2011; Hyndes et al. 2014).

Estuaries can be conceptualized as heterogenous habitats linked through interactions between river and tidal flows, which establish dynamic physiochemical gradients (e.g., salinity) along structurally stationary habitat features (e.g., vegetation communities, geomorphology), which in turn drive spatiotemporal variation in biological productivity and nekton community composition (Peterson 2003; Montagna et al. 2011; Hyndes et al. 2014) (Figure 1). As such, patterns of

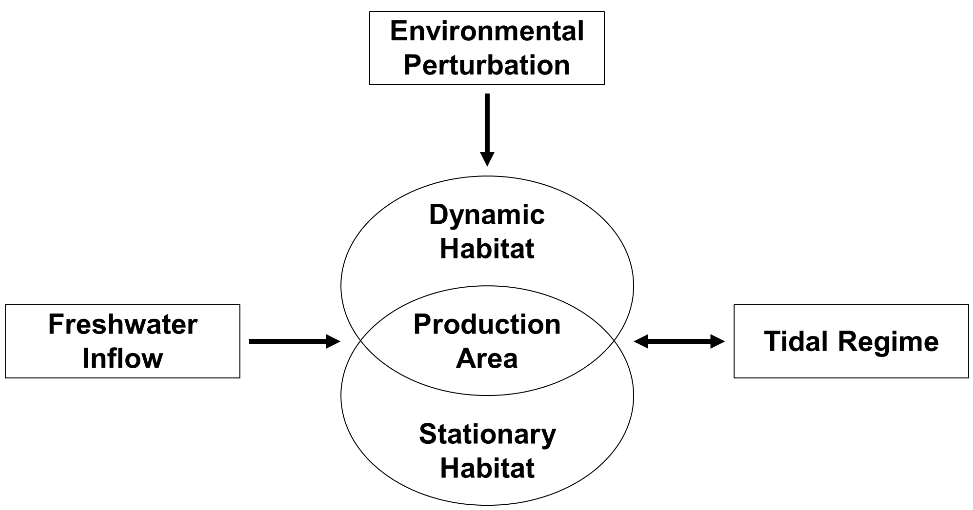

Figure 1. Conceptual model modified from Peterson (2003) displaying linkages of environmental components in estuarine ecosystems.

freshwater inflow and tides are considered key determinants of estuary function. Freshwater inflow from local terrestrial runoff, streams, and rivers facilitate several functional processes, such as input sources of nutrients, organic material, and sediment (Montagna and Kalke 1992; Montagna et al. 2011). Moreover, patterns of freshwater inflow influence salinity gradients. Tides also effect salinity, as well as promote connectivity within estuaries, resulting in the transport and exchange of organic material, energy, and fauna between different major habitat units (Sheaves and Johnston 2008; Rozas et al. 2013; Hyndes et al. 2014). To this end, long-term trends of freshwater inflow and tidal regimes govern the spatial configuration of structural habitat features, such as vegetation community composition, while short-term patterns dictate physiochemical gradients, connectivity, and energy exchange, which all in total drives changes in estuary function (Peterson 2003; Montagna et al. 2011; Hyndes et al. 2014).

Among these, freshwater inflows are recognized as a focal topic of research due to the increasing demand for water resources. Freshwater inflows fluctuate interannually and seasonally and the timing of inflows is important in structuring estuarine communities (Goberville et al. 2011). Therefore, variations in quantity and timing of freshwater inflow contributions can have both long-term and short-term effects on the organization of estuarine biota (Loneragan et al. 1989; Alber 2002; Palmer et al. 2011; Montagna et al. 2013). Natural climate patterns (e.g., drought) coupled with human utilization of water resources (e.g., storage, diversion) can alter hydrologic patterns of rivers (Steichen and Quigg 2018), thus influencing the timing and quantity of freshwater inflows into coastal estuarine systems (Longley 1994). The implementation of Senate Bill 3 revealed that major data gaps exist in the understanding of the role of freshwater inflows to bays and estuaries along the Texas Gulf Coast (BBEST 2011). In particular, there are limited ecological data at the interface between rivers and bays (i.e., tidal/delta areas), which are important nurseries for economically and ecologically important species within these estuarine areas (Longley 1994). Developing an understanding of functional relationships between freshwater inflows and biological productivity is an essential component for developing inflow recommendations for these understudied ecosystems (Alber 2002; Longley 1994; Quigg et al. 2009).

Therefore, the overarching goal of this study is to examine how dynamic and stationary habitats, including freshwater inflows and tidal regime, influence biotic communities and marsh productivity in the upper Guadalupe Estuary. Initial surveys were conducted in 2019 to establish baseline conditions of the vegetation and faunal assemblages within the Guadalupe Delta (BIO-WEST 2020). Continuation of seasonal monitoring was conducted in 2021, which included the initiation of avian community surveys (BIO-WEST 2022). Most recently, a third primary sampling period occurred from spring 2023 to winter 2024 with the addition of two new survey sites. This report summarizes results from all three primary sampling periods in 2019, 2021, and 2023-2024. Specific study objectives included: 1) assess intra- and inter-seasonal variation in vegetation communities; 2) evaluate spatiotemporal patterns in avian communities; 3) quantify environmental variation and its association with nekton community composition and assemblage structure; and 4) evaluate the effects of freshwater inflow and tidal regime on biological productivity.

2.0 METHODS

2.1 Study Area

The Upper Guadalupe Estuary consists of a series of interconnected bays, bayous, and riverine systems located at the mouth of the Guadalupe River in Refugio and Calhoun counties, Texas. This estuary represents the terminus of the Guadalupe-San Antonio River basin, receiving about 60% of its total freshwater inflow from the Guadalupe River drainage, with the remainder attributed to the San Antonio River and local drainages (Longley 1994; BBEST 2011). This study was conducted in the upper portions of this system (Figure 2) in marsh wetlands of the Guadalupe River Delta (hereafter 'the Delta'). Within the Delta, river flow splits into multiple channels and exhibits a complex hydrology dependent on flow conditions. During base flows, the majority of inflows drain into Mission Lake via Traylor Cut and Guadalupe Bay via the

Guadalupe River channel. Traylor Cut is a manmade channel that local authorities artificially trenched in 1935. This diversion of approximately two-thirds of the Guadalupe River freshwater discharge created additional wetlands habitat at the sub-delta that formed near its outlet into southwestern Mission Lake (Morton and Donaldson 1978). During flood events, there are greater contributions of inflow to Hynes Bay and the upper portion of San Antonio Bay (Longley 1994).

Three sites were established in 2019 to evaluate longitudinal trends in environmental conditions and biotic assemblages across the Delta. Site 1 was located near the mouth of the river's first outlet (Traylor Cut) at the southwestern edge of Mission Lake. Site 2 was located approximately mid-way between the river mouth and the tip of the Delta, within a marsh lake that drains into Guadalupe Bay via Redfish Bayou. Site 3 occurred at the most southern point of the Delta in the periphery of Lucas Lake, which is directly connected to the upper open-water portions of San Antonio Bay. In 2023, two new sites were established to assess biotic communities in different habitat types across the Delta. Site 4 was located near the mouth of Mamie Bayou at the northwestern edge of Misson Lake. Site 5 was established along the northern edge of Hynes Bay in an area directly adjacent to the mouth of Townsend Bayou (Figure 2).

2.2 Vegetation Community

Similar to previous vegetation community sampling, each site was visited twice, once in the spring (May) and once in the fall (November) of 2023. Number of transects, transect length, and number of plots per transect, however; were changed from 2019 to the remainder of the study period to increase sample sizes and provide a better representation of the marsh vegetation community. In 2021 and 2023, number of transects per site increased from 1 to 3, transect length was increased from 25 meters to 50 meters and number of temporal monitoring plots per transect was increased from 3 to 10. During sampling, a transect was established perpendicular to the shoreline at each site. The beginning of each transect started at the water's edge, at the time, and continued 50 meters (m) inland from the shoreline. Along each transect, 10 plots (1 m^2) were established for temporal monitoring of the vegetation community. At 5-meter intervals along the transect, plots were selected at a random distance from the transect line in a perpendicular direction, from 0–5 meters on either side.

For each temporal monitoring plot, dominant taxa, percent cover estimates for dominant taxa, and vegetation height were collected. Common and scientific names for wetland plants follow Stutzenbaker (1999). Plant species richness in the areas surrounding each transect was also recorded to help note the presence of species which may not have been captured in the transect plots. Standard water quality parameters (temperature [˚C], pH, dissolved oxygen [mg/L and percent saturation], specific conductance [µS/cm], and salinity [ppt]) were measured with a YSI ProDSS water-quality sonde in the water column at each site at the time of surveys.

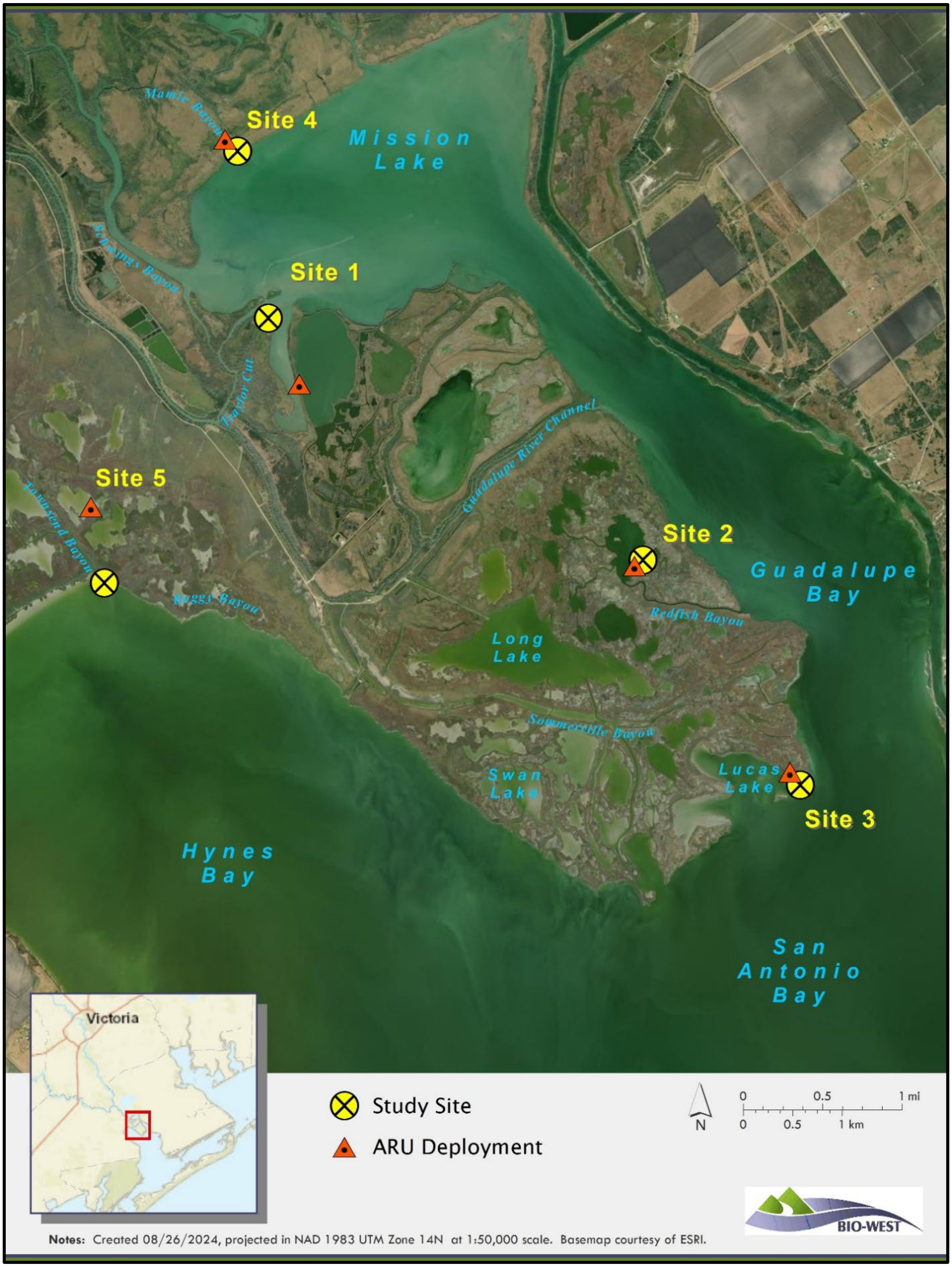

Figure 2. Location of study sites and automated recording units (ARU) for conducting seasonal ecological assessments at the Guadalupe River Delta (28.431, -96.795) in 2023 and 2024.

2.3 Avian Community

To evaluate avian communities across study sites and available habitats, timed point counts were conducted at each site during the spring (May), summer (August), and fall (November) of 2023 and winter (February) of 2024. Six timed point counts were conducted per site during each monitoring event to get representative samples among habitats present, including three counts located in proximity to emergent vegetated marsh edge (ME) and three in non-emergent vegetated bay bottom (SB). The selection of time point count locations occurred in the field at the time of each sampling event and was influenced by the seasonal variation in accessibility and availability of habitat types. Timed point counts were conducted for a fixed 10-minute period. During timed point counts, all avian species observed (identified either aurally or visually), number of individuals, habitat associations at the time of observation, and relevant climate parameters were recorded (Verner 1985; USDA 1997). Additionally, automated recording units (Song Meter SM4 Acoustic Recorder; Wildlife Acoustics, Inc.) were deployed and set to record continuously at each of the five sample sites over the entire study duration (Figure 2). Acoustic analysis focused on reviewing automated recordings for evidence of calling Eastern Black Rail (*Laterallus jamaicensis*) and Whooping Crane (*Grus americana*).

2.4 Nekton Community

Nekton assemblages were sampled within wadeable habitats using a 1 m^2 throw-trap (Figure 3), (Jordan et al. 1997; Rozas and Minello 1997; MBHE 2007). Surveys during the first two monitoring periods in 2019 and 2021 were conducted in summer and fall. Sampling at the third monitoring period occurred in the spring, summer, and fall of 2023 and winter 2024. At each monitoring period, marsh edge and open habitats were sampled within three transects per site during each seasonal event. A large dip-net was used to collect nekton in each throw-trap by sweeping it along the length of the substratum a minimum of 10 times. All nekton collected from each sample were fixed in 10% formalin, brought back to the BIO-WEST laboratory, identified to a practical taxonomic level, and enumerated. All fishes were measured to the nearest millimeter. Lastly, multiple habitat parameters were quantified within each throw-trap prior to nekton sampling. Temperature (˚C), pH, dissolved oxygen (DO) concentration (mg/L) and percent saturation (%), specific conductance (µS/cm), and salinity (ppt) were measured with a YSI ProDSS water-quality sonde. Emergent and submergent macrophyte coverage (%) was visually estimated and floating periphyton and vegetation were recorded as present or absent.

Figure 3. Throw-trap sampling at Site 1 during the spring 2023 monitoring event.

2.5 Data Analysis

All data analyses were performed with Microsoft Excel and the statistical programming environment R (version 4.2). Throw-trap data from all monitoring periods were used for nekton analysis. In addition to the habitat parameters quantified during throw-trap sampling, other data were obtained to characterize freshwater inflow and tidal regimes at the system-level. Tidal data were also used to approximate water levels during the time of sampling. Hourly tide level data (m; 2016-2024) was obtained from the nearest NOAA Tides and Current Monitoring Station (Seadrift, TX) as a proxy for water depth and the strength of marine-estuary interactions using the R package “rnoaa” (Chamberlain 2019).

Mean daily river discharge (cfs; 2000-2024) data were obtained from nearby USGS stream gages to provide approximations of freshwater inflows using the R package “dataRetrieval” (DeCicco 2022) (Table 1). Assessments of diversions and return flows were beyond the scope of this study and therefore not incorporated into estimates of freshwater inflow presented in this report. Freshwater inflows were estimated using similar methods to a recent assessment of historical freshwater inflows to the Guadalupe Estuary (HDR 2019). Estimates were based on the Guadalupe River near Tivoli when its mean daily discharge was ≤ 1,000 cfs. At mean daily discharges > 1,000 cfs, freshwater inflows were estimated based on the sum of select upstream gages to account for overbanking flows entering adjacent estuary drainages that are not captured by the Tivoli gage. For these high-flow periods, nearest upstream gages with available data are used and their respective travel times are corrected for to provide more accurate freshwater inflow estimates. As such, three different combinations of upstream gages were used (Table 1):

1) August 4, 2000 to November 24, 2005
    - Guadalupe River at Victoria
    - Coleto Creek near Victoria
    - San Antonio River at Goliad
2) November 25, 2005 to October 1, 2005
    - Guadalupe River at Victoria
    - Coleto Creek near Victoria
    - San Antonio River near McFaddin
3) October 2, 2005 to April 30, 2024
    - Guadalupe River near Bloomington
    - San Antonio River near McFaddin

Table 1. USGS stream gages used to estimate freshwater inflow in the Guadalupe Estuary from 2000 to 2024. The 1,000 cfs cutoff is based on mean daily river discharge at the Guadalupe River gage near Tivoli. When discharge at the Guadalupe River near Tivoli was greater than 1,000 cfs, freshwater inflows were estimated based on upstream gages in Guadalupe River and San Antonio River drainages to account for overbanking flows.

Gage #	**System**	**Location**	**Travel Time (days)**	**Start Date**	**End Date**
cfs ≤ 1,000					
08188800	Guadalupe River	Tivoli	0	2000-08-04	2024-04-30
cfs > 1,000					
08176500	Guadalupe River	Victoria	2	2000-08-04	2011-10-01
08177500	Coleto Creek	Victoria	2	2000-08-04	2011-10-01
08177520	Guadalupe River	Bloomington	1	2011-10-02	2024-04-30
08188500	San Antonio River	Goliad	2	2000-08-04	2005-11-24
08188570	San Antonio River	McFaddin	1	2005-11-25	2024-04-30

2.5.1 Environmental conditions

Time-series of mean daily river discharge and tide-level were used to illustrate freshwater inflow and tidal regimes over the duration of the study period and during discrete sampling periods. In addition, 90-day freshwater inflow and tide-level conditions were quantified to characterize recent regime trends prior to each sampling event using average as a magnitude index and two frequency indices. Low flow and high flow frequency were quantified as the number of days river discharge was less than Q10 (i.e., flows exceeded 90% of the time) and greater than or equal to Q90 (i.e., flows exceeded 10% of the time) magnitudes, respectively.

Principal components analysis (PCA) was performed using the R package "stats" (R-core package) to describe site-level differences in environmental conditions based on throw-trap data and tide level at the time of sampling. Continuous environmental variables were log transformed, proportional environmental variables were arcsine square root transformed, and categorical variables were coded as dummy variables. All continuous and proportional variables were also centered and scaled for analysis. Dissolved oxygen parameters were omitted from the PCA due to their strong correlation ($r > 0.7$) with time of day, meaning that potential spatial differences in DO are likely confounded and display variability in the sampling process rather than true site-level processes. Specific conductance was also removed from the PCA due to its strong correlation with salinity. Principal component loadings and mean (± standard deviation) PC scores of axes I and II were graphed to visualize spatiotemporal variation in environmental conditions. Environmental variables with PC loadings > |± 0.32| for the first two axes were considered meaningfully associated with a given component, meaning they represented > 10% of the variance in the PC (McGarigal et al. 2000).

2.5.2 Vegetation and avian communities

Vegetation community composition and percent dominance were calculated for each site. Once a species list was established, additional literature review was conducted to examine the salinity tolerance of the plant species observed to infer long-term patterns in typical salinity conditions at each site. Salinity tolerance values were based on data and information from Stutzenbaker (1999), Burdick and Konisky (2003), and USDA (2000).

For the assessment of the avian community, site and seasonal occurrence, taxa richness, relative abundance, and Shannon Diversity Index were calculated. Point counts were conducted within either emergent vegetated marsh or non-emergent vegetated bay bottom. However, given the radius of avian detectability (approximately 160-meters) and habitat heterogeneity present in the Delta, species were observed across five different habitat types. Therefore, species observations were reported by season, site, and associated habitat type including, emergent marsh, mudflat, open water, woodland, and shoreline. In addition, an avian taxa list per dominant habitat type per seasonal event was compiled. The software package Kaleidoscope Pro© (version 5.1.9; Wildlife Acoustics, Inc., Maynard, MA, USA) was used to analyze recorded audio data at each study site. Detection identification for Eastern Black Rail and Whooping Crane were based on classifiers that were previously developed and used for a similar project in Matagorda Bay (Stuntz et al. 2023). The project team ran the Kaleidoscope algorithm against our entire data set of field recordings by each study site, and then qualified observers manually reviewed every putative Eastern Black Rail and Whooping Crane detection identified by the classifier both aurally and visually (i.e., listening to the detection and inspecting the spectrogram, respectively).

2.5.3 Nekton community trends and habitat associations

Overall nekton taxa relative abundance (%), richness, and diversity were calculated for each site across all sampling events. Taxa diversity was calculated based on the Shannon Diversity Index (Shannon 1948). In addition, taxa were assigned to one of three estuary use guilds based on life history patterns and salinity tolerance for multiple analyses. Guilds included freshwater (i.e., freshwater obligate or migrants during spawning), estuarine-resident (i.e., complete life cycle in estuaries), and estuarine-dependent (i.e., reproduce offshore and occupy estuaries periodically as larvae/juveniles) (Day et al. 1989). Grass shrimp (*Paleon* sp.) were evaluated in aggregate due to the large numbers collected and difficulty in efficiently identifying to the species level. Overall site-level patterns in taxa richness, Shannon diversity, and relative abundance across estuary use guilds were compared using bar charts.

Nonmetric multidimensional scaling (NMDS) was used to visualize spatial dissimilarities in nekton assemblage structure, as well as to assess habitat associations with assemblage structure and taxa using the R package “vegan” (Oksanen 2022). Observations were aggregated for analysis by summing counts of each taxon by transect (n = 96) and were square root transformed. Taxa that occurred at two or less transects were omitted to limit the statistical influence of rare taxa that may have low detectability. The NMDS model was fit using Bray-Curtis dissimilarities based on transect-level abundance of nekton and specified two dimensions for analysis. Habitat variables were transformed the same as for PCA and fit as vectors to assess the influence of environmental variation on assemblage structure by quantifying correlation strength with site scores (i.e., transect). Habitat vectors were also compared with species scores to characterize taxa-habitat associations. Results of the NMDS were visualized based on mean (± standard deviation) site scores per study site, species scores, and habitat vectors for axes I and II.

2.5.4 Effects of freshwater inflow and tidal regimes

Generalized linear mixed effects models were fit using the R package ‘glmmTMB’ (Brooks 2024) to estimate effects of freshwater inflow and tidal regimes on nekton density as an indicator of potential determinants on marsh biological productivity. Density of each estuary use guild was summed for each throw-trap sample for analysis. Exploratory data analysis was first conducted to select an index (i.e., average, low pulse frequency, high pulse frequency) and rolling statistic (i.e., 30-day, 90-day, 180-day, 1-year) for representing freshwater inflow and tide covariate effects.

Data pre-processing and preliminary model fitting resulted in the following model structure: 1) error distribution – negative binomial with quadratic parameterization for overdispersion (Linden and Mantyniemi 2011); 2) fixed effects – 180-day high flow pulse frequency (# days) covariate and 90-day average tide-level (m) covariate fit with a quadratic term; 3) dispersion sub-model with covariates – salinity and total vegetation coverage (%) covariates; and 4) random effects – site and estuary use guild group-level predictors and observation-level random effects (i.e., individual throw-trap samples) that represents an extra-dispersion term (Harrison 2014). All covariates were centered for analysis.

Predictive performance of the full model was assessed and compared with alternately structured models using the R package ‘performance’ (Lüdecke 2024a). Alternate models included fixed effects only, fixed effects and dispersion sub-model with covariates, and fixed effects and random effects, which were compared based on Akaike Information Criteria (AIC), Bayesian Information Criteria (BIC), and root mean squared error (RMSE). For the full model, conditional R^2 and residual standard deviation were also calculated to further assess goodness-of-fit. Parameter estimates and associated 95% confidence intervals (CI) for the full model were obtained using the R package ‘parameter’ (Lüdecke 2024b) and marginal effects of 90-day high flow pulse frequency and 90-day average tide level on nekton density were visualized using the R package ‘ggeffects’ (Lüdecke 2024c). Lastly, random effects coefficients for each site and estuary use guild group-level were calculated and visualized to compare against the fixed effects intercept estimate using the R package ‘modelbased’ (Makowski 2024).

3.0 RESULTS

3.1 Vegetation Community

3.1.1 Community Composition

Across all five sampling sites, the vegetation community was typical of low-lying tidal marsh areas that experience varying levels of inundation. Based on measurements recorded during each sampling event, salinity conditions varied across sites. Site 1 consisted of oligohaline conditions, Site 2 and Site 4 represented mesohaline conditions, and Site 3 and Site 5 were characterized by polyhaline conditions (Table 2). The marsh vegetation at Site 1 was generally dominated by broad leaved herbaceous species. Sites 2, 3, and 5 were dominated by graminoid species with less dominant herbaceous and shrub species. Site 4 was dominated by a mixture of graminoid, herbaceous, and shrub species. When comparing 2023 data to previous years, it is important to note that the study was expanded in 2021 to increase sample size and better characterize the community composition. While 2021 and 2023 transects at sites 1, 2, and 3 overlap with 2019 transects, they are slightly different due to the expansion. Additionally, two new sites (sites 4 and 5) were added in 2023. Similar to observations from 2021 sampling, species overlap among sites was relatively high with Alkali Bulrush (*Bolboschoenus maritimus*) and Sea Myrtle (*Baccharis halmifolia*) found across four sites and Wiregrass (*Spartina patens*) observed across 3 sites.

Table 2. Average salinity (ppt) recorded at each site during each vegetation sampling event (denoted ‘a’) in spring and fall, average salinity during nekton sampling (denoted ‘b’) in summer and winter, and salinity point measurements during monthly auditory data retrieval events (denoted ‘c’).

	Site				
Month	**1**	**2**	**3**	**4**	**5**
2023					
May[a]	0.25	1.65	0.92	0.25	1.73
June[c]	0.41	4.25	5.71	0.37	6.34
July[b]	0.44	10.52	11.17	0.47	12.62
August[c]	0.58	12.64	14.65	1.58	16.13
September[c]	9.10	24.80	25.92	11.00	27.40
October[c]	2.12	20.07	22.10	14.51	26.25
November[a]	0.46	16.44	26.23	8.65	24.18
December[c]	3.14	21.06	24.72	17.51	24.62
2024					
January[c]	0.26	10.75	5.85	3.00	4.64
February[b]	0.24	3.47	1.64	0.41	6.69
March[c]	0.48	6.37	0.17	2.97	9.32
April[c]	0.41	8.42	10.95	0.41	10.59

In 2023, Site 1 primarily consisted of herbaceous aquatic species. A total of 12 species were documented, representing the second highest species richness among sites. The spring consisted of a more diverse community than the fall. In the spring, 12 species were present and dominant species included two exotic species, Water Hyacinth (*Hydrocotyle bonariensis*) and Alligatorweed (*Alternanthera philoxeroides*), and two native species, Broadleaf Arrowhead (*Sagittaria latifolia*) and Climbing Hempweed (*Mikania scandens*). In the fall, the vegetation community shifted from aquatic, herbaceous species to graminoid species (e.g., Sawgrass *Zizania miliacea*). Other species such as Southern Cattail (*Typha domingensis*) and the exotic Wild Taro (*Colocasia esculenta*) also increased in dominance in the fall.

Sites 2 and 3 had the lowest species diversity in 2023, with 4 species identified from sampling plots. The community was comprised mostly of graminoid species, such as rushes and grasses, and a couple herbaceous species (Table 3). Site 2 was dominated by facultative halophytes which have wide salinity tolerances suggesting that they can inhabit areas that experience occasional freshwater inputs while also tolerating sustained saline conditions. At Site 2, Wiregrass and Alkali Bulrush dominated the community across both seasons. While Alkali Bulrush and Sea Myrtle decreased in dominance from spring to fall, Wiregrass and Saline Aster increased.

The community at Site 3 consisted of Alkali Bulrush, Common Reed, Sea Myrtle, and Wiregrass (Table 3). Across both seasons in 2023, Sea Myrtle, a woody shrub species, was dominant at Site 3 and observed as a thick stand along the bank. This contrasts with 2019 sampling in which the site was largely composed of a homogenous stand of Smooth Cordgrass and with 2021 sampling in which the site was dominated by Saltmarsh Bulrush. Similar to previous years, this site was noted as having the largest variation in salinity between spring and fall sampling events, ranging from 0.92 to 26.23, respectively (Table 2). The wide salinity tolerance of Smooth Cordgrass (5 to 35 ppt) suggests that another factor (e.g., depth, flooding duration) might contribute to the decline in dominance, although it should be noted that small patches of Smooth Cordgrass were still observed outside of the transects at Site 3 in 2023. In contrast, the narrower salinity tolerance of Saltmarsh Bulrush (3.5 to 10 ppt) might have contributed to its decline in dominance since 2021, given the wide variability in salinity from spring to fall.

Site 4 had the highest species richness among sites, with 15 species documented in 2023. This community was composed of a mix of shrub, herbaceous, and graminoid species (Table 3). The Common Reed (*Phragmites australis*) was the most dominant species at Site 4 during both sampling seasons, followed by Saline Aster (*Aster tenuifolius*). Several less common species were observed throughout the community including Buttonbush (*Cephalanthus occidentalis*), Hedge Bindweed (*Calystegia sepium*), Sea Myrtle, Sea Oxeye (*Borrichia frutescens*), Sawgrass (*Zizaniopsis miliacea*), Shoregrass (*Monanthochloe littoralis*), Spider Lily (*Hymenocallis liriosme*), and Swamp Lily (*Crinum americanum*). The community transitioned from obligate wetland plants (e.g., Saline Aster) along the bank to facultative plants (e.g., Sea Myrtle) along the upper fringes of the marsh. By fall, Common Reed dominance increased, and species richness declined to 5 species.

Site 5 consisted of 9 species across the spring and fall of 2023 (Table 3). This site was dominated by a mixture of graminoid and shrub species such as Gulf Cordgrass (*Spartina spartinae*) and Sea Oxeye. Site 5 was characterized by a shift from shrub to graminoid species as the transects transitioned from the Towsend Bayou channel toward the inner marsh. The woody shrub species Sea Myrtle was dominant near the bank along the Townsend Bayou channel. Sea Myrtle transitioned to Gulf Cordgrass followed by Sea Oxeye, Turtleweed (*Batis maritima*) and

Shoregrass. Additionally, Carolina Wolfberry (*Lycium carolinianum*), a notable food source for the Whooping Crane, was also present at this site in spring and fall.

Table 3. Percent dominance of plant species identified from sampling plots at five sites in the Guadalupe Delta during spring (S; May) and fall (F; November) 2023.

	Site 1		**Site 2**		**Site 3**		**Site 4**		**Site 5**	
Species	**S**	**F**	**S**	**F**	**S**	**F**	**S**	**F**	**S**	**F**
Alkali bulrush	-	-	39	24	25	14	4	0	3	3
Alligatorweed	20	8	-	-	-	-	-	-	-	-
Broadleaf Arrowhead	15	0	-	-	-	-	-	-	-	-
Buttonbush	-	-	-	-	-	-	6	0	-	-
Carolina Wolfberry	-	-	-	-	-	-	-	-	5	8
Climbing Hempweed	13	0	-	-	-	-	2	0	-	-
Coast Barnyard Grass	<1	0	-	-	-	-	-	-	-	-
Common Reed	-	-	-	-	17	23	47	75	-	-
Delta Arrowhead	5	0	-	-	-	-	-	-	-	-
Flat Sedge	-	-	-	-	-	-	<1	0	-	-
Gulf cordgrass	-	-	-	-	-	-	-	-	24	12
Hedge bindweed	-	-	-	-	-	-	4	0	-	-
Knotweed	2	0	-	-	-	-	-	-	-	-
Marsh Pennywort	1	0	-	-	-	-	2	0	-	-
Saline aster	-	-	8	17	-	-	13	11	-	-
Sawgrass	2	49	-	-	-	-	4	8	-	-
Sea Myrtle	-	-	4	0	47	42	6	1	23	13
Sea oxeye	-	-	-	-	-	-	1	0	24	10
Seashore dropseed	-	-	-	-	-	-	-	-	0	22
Shoregrass	-	-	-	-	-	-	4	0	8	0
Smooth Beggartick	9	0	-	-	-	-	-	-	-	-
Southern Cattail	<1	21	-	-	-	-	-	-	-	-
Spider lily	-	-	-	-	-	-	3	<1	-	-
Swamp lily	-	-	-	-	-	-	2	0	-	-
Swamp smartweed	-	-	-	-	-	-	1	0	-	-
Turtleweed	-	-	-	-	-	-	-	-	10	15
Water Hyacinth	31	0	-	-	-	-	-	-	-	-
Wild Taro	2	21	-	-	-	-	-	-	-	-
Wiregrass	-	-	48	59	5	26	-	-	2	17

All sites were characterized by lower salinity in the spring compared to fall with sites 2, 3, and 5 demonstrating large increases in salinity from spring to fall (Table 2). Inflow conditions are likely a driver for wide salinity variations given that above average rainfall throughout the watershed occurred in April 2023 prior to sampling in May. This is further evidenced by data collected in 2021, in which a large decrease in salinity was observed between spring and fall events at Sites 2 and 3. In 2021, above average rainfall throughout the watershed was observed in

May, June, July, September, and October prior to sampling in November. Furthermore, the plant community across sites with the largest fluctuation in salinity are characterized as moderate to high saline tolerant species, suggesting that low salinities at these sites might be an atypical situation.

3.1.2 Salinity Tolerance

To further explore salinity tolerance of the species observed, additional literature review was conducted to examine the range of salinity tolerance reported for the dominant species at each site. Only plant species with available data were included. Reported ranges demonstrated that the plant community present at Site 1 is mostly intolerant of salinity. The community at Site 4 varied from low to moderate salinity tolerance. Sites 2, 3, and 5 exhibited a wider variation in salinity tolerance and primarily varied between moderate to high tolerance (Figure 4). Trends for sites 1, 2, and 3 are consistent with those reported during 2019 and 2021 sampling.

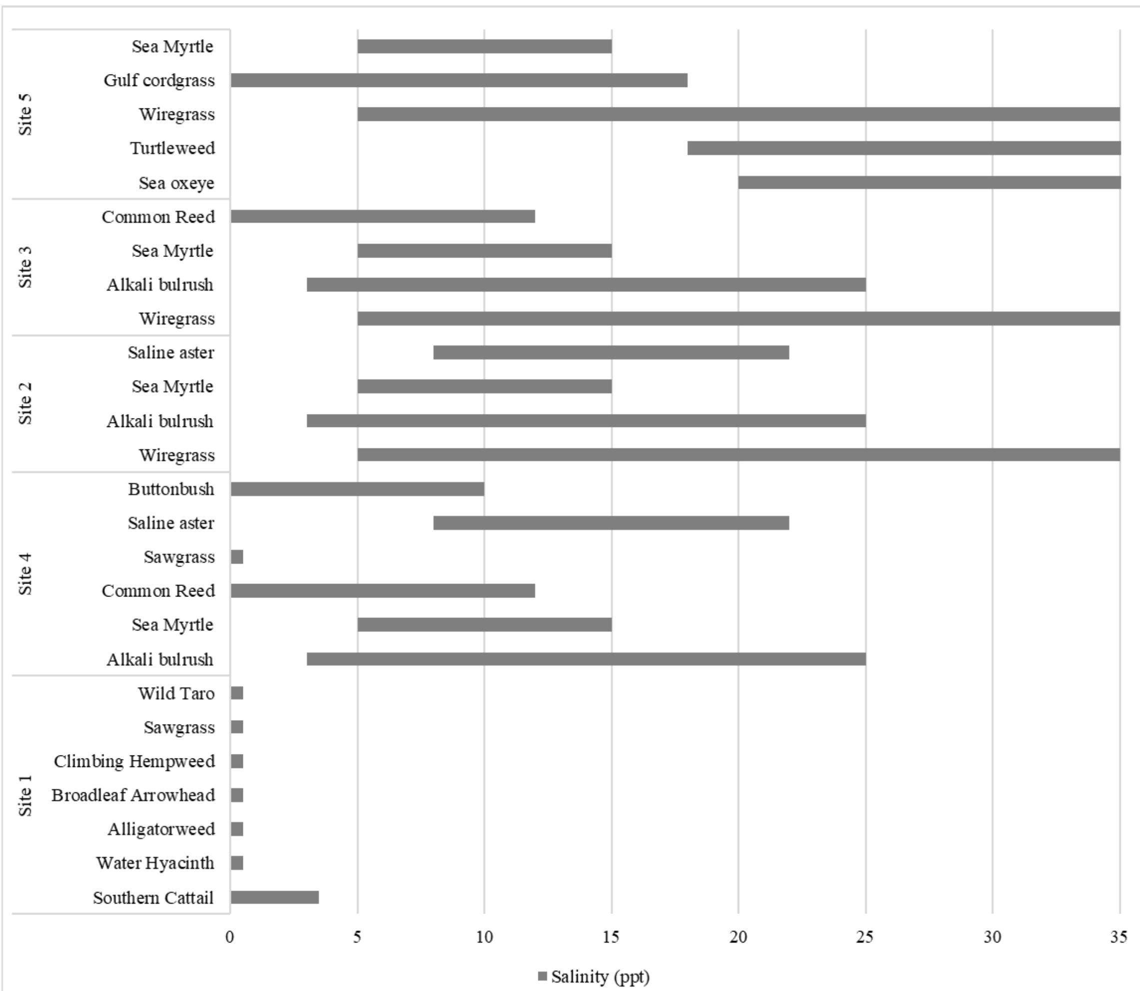

Figure 4. Reported salinity tolerance ranges for observed dominant species at each site in 2023. Salinity tolerances are based on data and information from Perry & Atkinson 1997, Stutzenbaker 1999, USDA 2000, and Burdick and Konisky 2003.

3.2 Avian Community

In total, 4,341 individuals represented by 112 taxa were observed during seasonal sampling events in 2023 and 2024 (Table 4). Avian results in Table 5 include species that accounted for ≥ 1% of all individuals observed (and the endangered Whooping Crane) and complete summaries of these data can be found in the Appendix. The avian community was typical of an ecosystem presenting a mosaic of saltwater influenced marsh, shoreline, and mudflat habitat. All sites were characterized by an abundance of shorebird and/or migratory bird species, with relatively high species overlap between sites (Table 5). Percent relative abundance was relatively even across sites, ranging from 15.4% at Site 2 to 23.1% at Site 5. Taxa richness was highest at Site 1 (58 taxa), Site 2 (57 taxa), and Site 3 (58 taxa), followed by Site 5 (54 taxa) and Site 4 (49 taxa). Despite Site 1 being taxa rich, it along with Site 4 were the least diverse (2.47 and 2.30, respectively). Shannon diversity was higher and relatively similar at the remaining sites (3.28-3.34) (Table 4).

Table 4. Avian count (#), taxa richness (#), relative abundance (%), and Shannon diversity by site.

Site	Count	Taxa Richness	Relative Abundance (%)	Shannon Diversity
1	928	58	21.4	2.47
2	668	57	15.4	3.28
3	902	58	20.8	3.34
4	840	49	19.4	2.30
5	1003	54	23.1	3.23
Total	4341	112	-	-

The overall community was not dominated by any particular taxa, though four species represented about 40% of all individuals, which included Red-winged Blackbird (10.7%), Cattle Egret (10.1%), Brown Pelican (10.1%), and Boat-tailed Grackle (9.5%). A total of 22 species were ubiquitously observed across the Delta that included Pelecaniformes (e.g., Brown Pelican, Double-crested Cormorant), wading birds (e.g., Great Blue Heron, Roseate Spoonbill), diurnal raptors (e.g., Northern Harrier, Osprey), gulls and terns (e.g., Laughing Gull, Royal Tern), two icterids (i.e., Boat-tailed Grackle, Red-winged Blackbird), one Gruiformes (i.e., Common Gallinule), and one wood-warbler (i.e., Common Yellowthroat). Moreover, 11 and 10 taxa were unique to Site 2 and Site 3, respectively, most of which were shorebirds (e.g., Greater Yellowlegs, Spotted Sandpiper). Both Site 1 and Site 4 harbored 7 unique taxa, representing a variety of taxonomic groups. Lastly, 5 taxa were only detected at Site 5 including the endangered Whooping Crane. A total of 8 Whooping Cranes were observed within emergent marsh habitat during winter 2024 (Table 5).

Table 5. Overall count (#) and relative abundance (%), relative abundance across seasons and sites, and detection across dominant habitat types for the avian communities observed during sampling in 2023 and 2024. Habitat types included emergent marsh (EM), mudflat (MF), open water (OW), woodland (WL), and shoreline (SL).

	Total		**Season (% relative abundance)**				**Site (% relative abundance)**					**Habitat Use (x = detected)**				
Taxa	**#**	**%**	**Spring**	**Summer**	**Fall**	**Winter**	**1**	**2**	**3**	**4**	**5**	**EM**	**MF**	**OW**	**WL**	**SL**
American Avocet	92	2.12	0.0	0.0	9.8	90.2	3.3	16.3	63.0	0.0	17.4	x	x	x		x
Boat-tailed Grackle	411	9.47	63.3	24.6	11.7	0.5	15.1	21.4	16.1	18.2	29.2	x		x	x	
Brown Pelican	437	10.07	0.0	0.5	98.9	0.7	0.7	0.7	6.2	89.2	3.2			x		x
Canada Goose	48	1.11	0.0	0.0	100.0	0.0	100.0	0.0	0.0	0.0	0.0					
Cattle Egret	440	10.14	48.2	51.6	0.2	0.0	88.4	2.5	0.2	7.7	1.1	x				
Common Tern	173	3.99	39.3	51.4	2.3	6.9	3.5	5.8	50.9	4.0	35.8	x	x	x		
Double-crested Cormorant	82	1.89	13.4	2.4	30.5	53.7	14.6	29.3	13.4	1.2	41.5	x		x		
Dowitcher sp.	78	1.80	0.0	0.0	0.0	100.0	0.0	6.4	41.0	0.0	52.6		x			x
Great Blue Heron	69	1.59	20.3	2.9	40.6	36.2	11.6	27.5	20.3	8.7	31.9	x	x	x		x
Laughing Gull	122	2.81	9.8	18.9	37.7	33.6	4.1	13.1	28.7	4.1	50.0	x	x	x		
Least Sandpiper	59	1.36	0.0	32.2	0.0	67.8	0.0	61.0	37.3	0.0	1.7	x	x			x
Orange-billed Skimmer	58	1.34	0.0	0.0	0.0	100.0	0.0	0.0	100.0	0.0	0.0		x			
Red-winged Blackbird	464	10.69	60.6	8.2	15.7	15.5	24.4	25.0	20.7	7.1	22.8	x		x	x	x
Ring-billed Gull	82	1.89	0.0	0.0	74.4	25.6	0.0	0.0	18.3	0.0	81.7		x	x		
Roseate Spoonbill	49	1.13	12.2	38.8	20.4	28.6	40.8	8.2	14.3	2.0	34.7	x				
Royal Tern	60	1.38	6.7	8.3	58.3	26.7	13.3	3.3	33.3	1.7	48.3	x	x	x		x
Scaup sp.	120	2.76	0.0	0.0	0.0	100.0	0.0	0.0	20.0	0.0	80.0		x			
Snowy Egret	78	1.80	34.6	24.4	25.6	15.4	9.0	30.8	24.4	20.5	15.4	x	x	x		x
Tree Swallow	53	1.22	0.0	0.0	100.0	0.0	0.0	0.0	15.1	0.0	84.9	x				
Tricolored Heron	44	1.01	65.9	25.0	6.8	2.3	45.5	20.5	15.9	6.8	11.4	x		x		
Turkey Vulture	96	2.21	1.0	2.1	69.8	27.1	6.3	18.8	33.3	34.4	7.3	x		x		x
White Ibis	56	1.29	21.4	39.3	8.9	30.4	25.0	21.4	28.6	10.7	14.3	x	x			x
White Pelican	97	2.23	0.0	1.0	15.5	83.5	1.0	1.0	68.0	0.0	29.9		x			
Whooping Crane	8	0.18	0.0	0.0	0.0	100.0	0.0	0.0	0.0	0.0	100.0	x				
Yellow-rumped Warbler	126	2.90	0.0	0.0	45.2	54.8	36.5	0.0	0.0	63.5	0.0	x			x	

Automated recording units collected auditory data from May 2023 to May 2024 for a total of 991.1 hours logged. Data processing resulted in 459,447 detections, of which the classifier automatically identified 67,255 putative detections (14.64% of total detections) across all five sites. Manual review of putative detections by project team biologists found all detections were false-positive detections and not true Eastern Black Rail or Whooping Crane calls (Table 6).

Table 6. Summary of automated acoustic analysis of Eastern Black Rail and Whooping Crane field recordings at five sites in the Guadalupe River Delta.

Site	Hours Logged	Output Detections	Putative Detections (%)	Black Rail True Detections	Whooping Crane True Detections
Site 1	77.8	30,009	758 (2.53%)	0	0
Site 2	50	39,816	4,611 (11.58%)	0	0
Site 3	50.1	15,783	1,005 (6.37%)	0	0
Site 4	77.1	22,885	2,985 (13.04%)	0	0
Site 5	44.4	20,553	2,782 (13.54%)	0	0
Total	**991.1**	**459,447**	**67,255 (14.64%)**	**0**	**0**

3.3 Nekton Community

3.3.1 Environmental conditions

Freshwater inflow and tidal regimes

Freshwater inflow conditions were 196-310 cfs above the long-term (2000-2024) median (1,240 cfs) during sampling periods in summer 2019, fall 2021, and spring 2023. In contrast, freshwater inflows were 290-927 cfs below the long-term median in fall 2019, summer 2013, and fall 2023. In addition, inflows during summer 2023 closely approximated Q10 river discharge (473 cfs). Freshwater inflows during sampling in summer 2021 and winter 2024 were 752-1,560 cfs greater than the long-term median, representing Q68 and Q78 inflow magnitudes, respectively. Mean daily tide-level showed a seasonal pattern, being lowest in winter and highest in spring and fall, ranging from 0.31-0.75 m. Tide-level was lowest in winter 2024 (0.31-0.38 m), at levels below Q10 tide-level (0.40 m), and was highest in fall and spring 2023 (0.72-0.75 m) (Figure 5).

Recent 90-day trends in freshwater inflow and tidal indices varied among sampling periods and demonstrated dynamic, and sometimes cyclical, regimes. No freshwater inflow indices correlated with tide-level indices ($r < |0.50|$). The 90-day average river discharge flow index displayed a strong negative correlation with Q10 low flow pulse frequency ($r = -0.71$) and Q90 high flow pulse frequency ($r = 0.94$). Similarly, 90-day average tide-level was strongly correlated negatively with Q10 ($r = -0.86$) and positively with Q90 ($r = 0.87$) pulse frequency (Figure 5; Table 7).

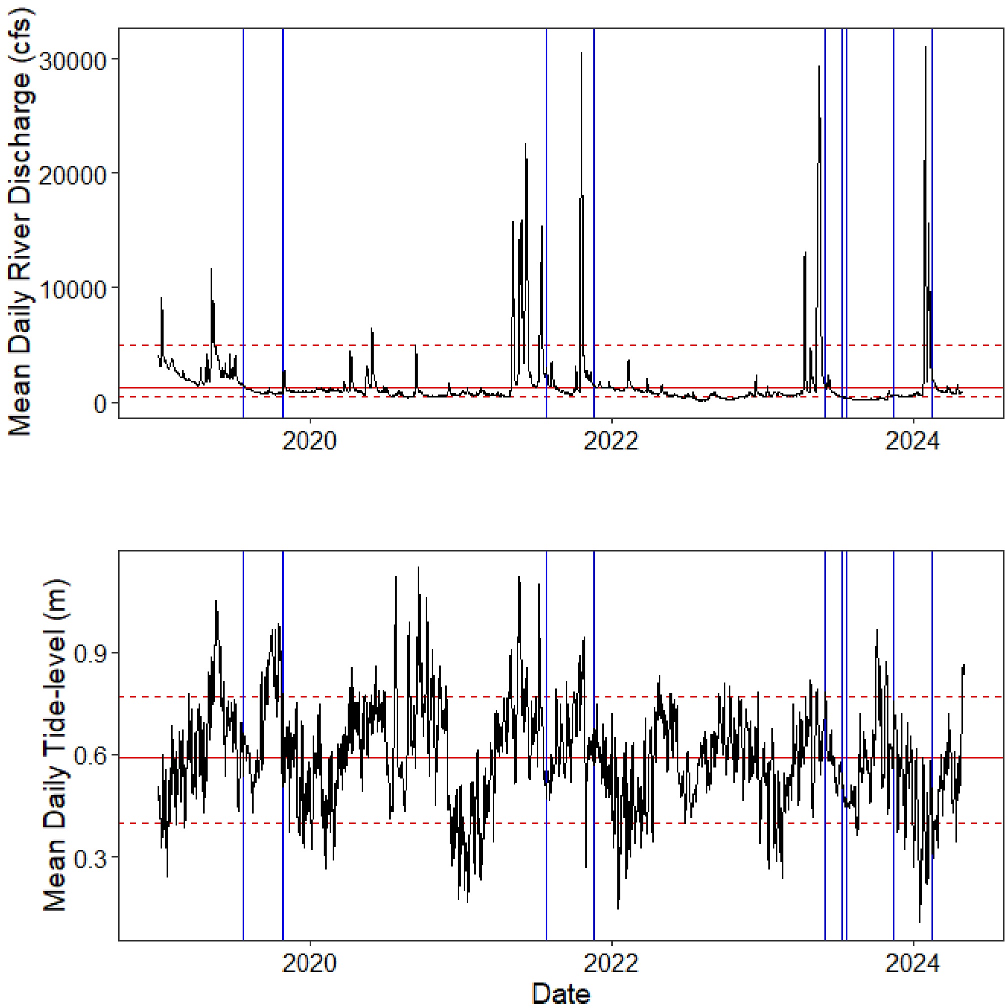

Figure 5. Time-series displaying mean daily river discharge (cfs) and tide-level (m) during ecological assessments in the Guadalupe River Delta from 2019-2024. Blue vertical lines denote nekton community sampling periods the solid red line represents the long-term (2000-2024) median (1,240 cfs, 0.59 m), and dashed red lines are Q10 (473 cfs, 0.40 m) and Q90 (4,945 cfs, 0.77 m) magnitudes.

The 90-day average river discharge flow index was above the long-term median (1,240 cfs) for most sampling events (~2,100-4,800 cfs). Patterns of both 90-day average and Q90 frequency illustrated seasonality. In 2019 and 2021, both indices were higher in summer (~3,100-4,800 cfs, 8-26 days) than fall (~880-2,200 cfs, 0-4 days), and in 2023, decreased from spring (~3,700 cfs, 16 days) to fall (~330 cfs, 0 days), then increased again in winter 2024 (~4,800 cfs, 10 days). The Q10 low flow frequency index displayed a discontinuous trend, with frequencies generally being low (0-11 days) other than a large increase in fall 2023 (74-75 days) when average discharge was lowest. In addition, 90-day average tide-level decreased from summer 2019 (0.72 m) to winter 2024 (0.46 m) and Q10 frequency was 2 days or less except in winter 2024 (32-33 days). The 90-day Q90 tide-level index showed a similar trend to the 90-day average, remaining relatively high from fall 2019 to fall 2021 (18-37 days), and decreased up to winter 2024 (0 days) (Table 7).

Table 7. Indices summarizing recent 90-day mean daily river discharge (FWI; cfs) and tide-level (TL; m) during survey efforts within nekton community sampling periods in the Guadalupe River Delta from 2019-2024. 90-day Q10 magnitudes were 473 cfs and 0.40 m. Q90 magnitudes were 4,945 cfs and 0.77 m.

	Magnitude		**Frequency**			
	90-day Average		**90-day Q10**		**90-day Q90**	
Sampling Period	**FWI**	**TL**	**FWI**	**TL**	**FWI**	**TL**
Summer 2019	3,164-3,170	0.72	0	0	8	27
Fall 2019	880-882	0.71	0	0	0	37
Summer 2021	4,779-4,803	0.72-0.73	0	0	26	27-28
Fall 2021	2,161-2,162	0.67	0	2	4	18-19
Spring 2023	3,727-3,737	0.62-0.63	0	0	16	7
Summer 2023	3,279-3,387	0.60-0.62	2-11	0	12	8
Fall 2023	327-332	0.62-0.63	74-75	1	0	14
Winter 2024	2,763-2,779	0.46	2	32-33	10	0

Site-level environmental variation

Principal component axes I and II explained 23.4% of the variation in environmental parameters among 390 throw-trap samples during eight events. Axis I explained 13.7% of the variation and described a salinity and vegetation gradient. Meaningful PC loadings for axis I were Duckweed (0.50), Water Hyacinth (0.47), and salinity concentration (-0.38). Axis II explained 9.7% of the variation and described a water chemistry gradient, with meaningful PC loadings being represented by pH (-0.58) and water temperature (-0.61) (Figure 6).

Ordination of mean sample scores across sites displayed two general subgroups that included Site 1 versus Site 2-5. Principal Component I distinguished Site 1 from other sites based on salinity and vegetation composition. Salinity concentrations were lowest at Site 1 (0.23 – 0.74 ppt) and ME habitats had high coverage of water hyacinth (median = 70.0%) and duckweed (family: Lemnoidae), which were absent at the other sites. The large standard deviation for PC I at Site 1 was attributed to variation in vegetation available in both edge and open habitats. Dissimilarities between Site 2 – 5 were best explained by salinity regimes, with lower variation observed at Site 4 (0.23 – 10.11 ppt) compared to Site 2 (0.62 – 17.00 ppt), Site 3 (0.76 – 27.04 ppt), and Site 5 (1.16 – 24.24 ppt) (Figure 6).

Principal Component II displayed seasonal differences in water temperature across all sites, which were lowest in winter (16.1-23.3 °C) and greatest in summer (25.7-37.3 °C). Site-level differences in pH were also apparent along PC II and were highest during summer at Site 2 (8.09-9.76) and Site 3 (8.36-10.10). Moreover, median tide level was higher during fall sampling in 2019 (0.24-0.37 m) and 2021 (0.24-0.37 m). In summer, tide level was higher in 2019 (0.12-0.15 m) compared to 2021 (0.03-0.10 m). Vegetation taxa at Site 2, Site 3, and Site 5 were not strongly associated with either PC axis, which was best explained by median tide level during sampling (Figure 6). Specifically, percent vegetation cover in ME habitats was at or near zero when tide level was less than 0.50 m. Vegetation cover was minimally available at Site 4 (max = 5%).

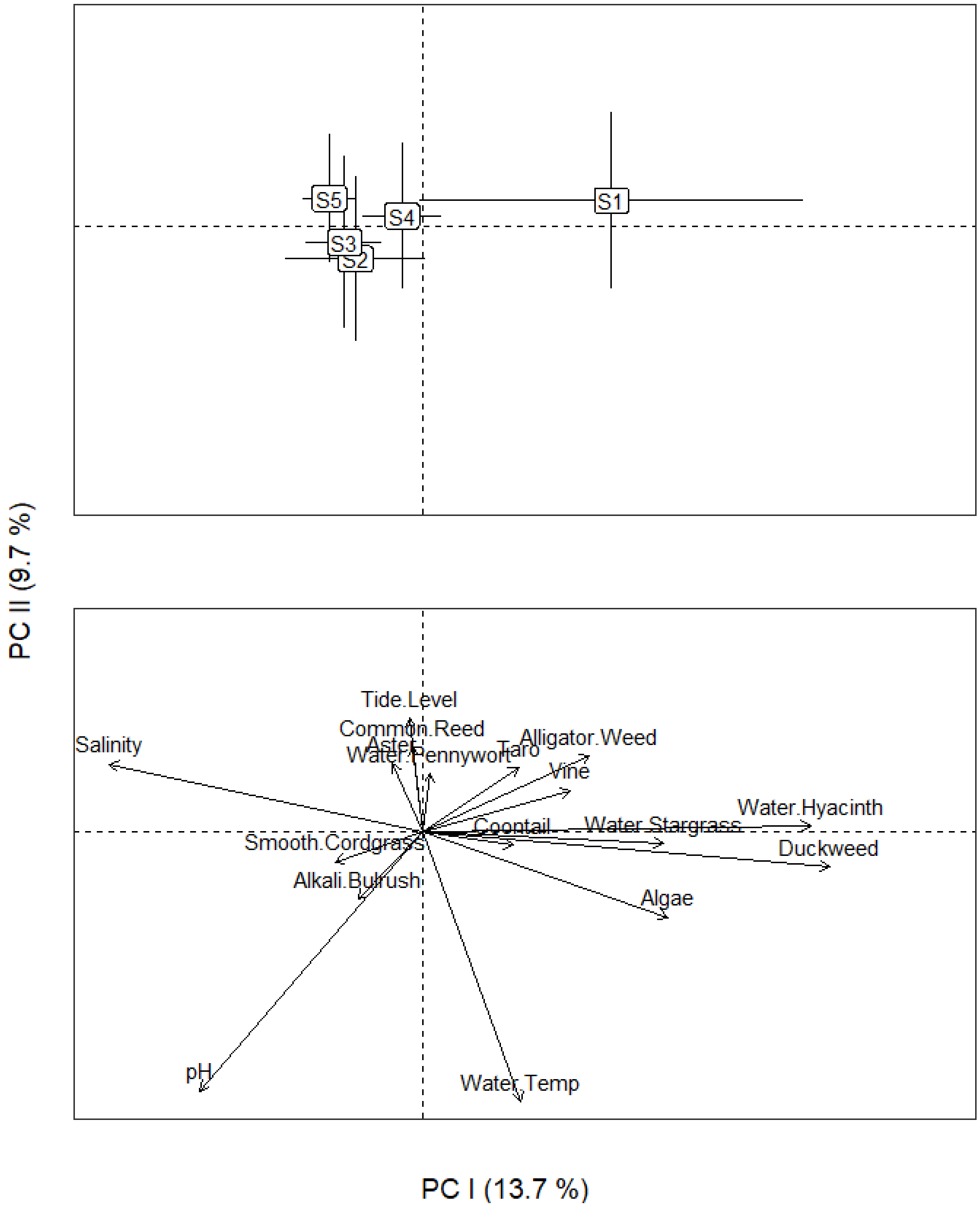

Figure 6. Principal components analysis bi-plots displaying mean (± standard deviation) sample scores (top panel) and PC loadings of environmental variables (bottom panel) among five sites (S1–S5) sampled at the Guadalupe River Delta in 2019, 2021, 2023, and 2024.

3.3.2 Community trends and habitat associations

General community trends

A total of 18,306 individuals represented by 31 families and 64 taxa were observed over the entirety of the study. Nekton results in Table 8 include taxa that accounted for ≥ 0.1% of the community in at least one site and complete summaries of these data can be found in the Appendix. Overall taxa richness was highest at Site 1 (44 taxa), Site 2 (31 taxa), and Site 3 (29 taxa). In contrast, Shannon diversity was greater at Site 2 (1.76) and Site 3 (1.58) than Site 1 (1.37). Shannon diversity was also high at Site 5 (1.72), despite lower taxa richness (24 taxa). Site 4 displayed the lowest taxa richness (17 taxa) and diversity (0.84) (Table 8).

Among estuary use guilds, freshwater taxa richness and Shannon diversity were substantially higher at Site 1 (18 taxa and 2.07, respectively) compared to Site 2 and 3 (2-3 taxa and 0.56-0.64, respectively) and no freshwater nekton were observed at Site 5. Site 4 had a lower number of freshwater taxa (6 species), yet Shannon diversity (1.79) was similar to Site 1. In addition, estuarine-resident richness and diversity were greatest at Site 1 (18 taxa and 0.95, respectively) and Site 2 (16 taxa and 1.48, respectively). Site 2 also displayed high estuarine-dependent richness (11 taxa) and diversity (1.69). Taxa richness at Site 3 and Site 5 were similar between resident (11-12 taxa) and dependent (12-15 taxa) estuary users, though Shannon diversity was substantially higher for estuarine-dependent taxa (1.53-1.73) than estuarine-resident taxa (0.54-0.66). Lastly, both estuarine-resident and -dependent richness (5-6 taxa) and diversity (0.32-0.87) were relatively low at Site 4 (Figure 7).

Higher freshwater diversity at Site 1 and Site 4 was due to multiple unique freshwater fish species only being documented at Site 1 (n = 12 taxa; e.g., Golden Topminnow, Bantam Sunfish) and Site 4 (i.e., Florida/Largemouth Bass, Red Shiner). Other unique taxa included Hogchoker, Snook, and Spotfin Mojarra at Site 1 and Skipjack Herring at Site 4. Similarly, higher estuarine-dependent diversity at Site 3 was partially due to multiple species only being documented at this location (e.g., Skilletfish, Speckled Worm Eel). Surprisingly, two freshwater taxa were only observed at Site 3 (i.e., Big Claw River Shrimp, Blue Catfish). In contrast, only one unique taxon was observed at Site 2 (i.e., Black Drum) and Site 5 (i.e., Flagfin Mojarra) and higher diversity of estuary residents and dependents at these locations were instead due to relatively more even taxa composition compared to other sites (Table 8; Figure 7).

Relative abundance of estuarine-residents dominated nekton assemblages and accounted for ~75% of individuals at all sites except Site 5, which displayed more even relative abundances between estuarine-resident (46.6%) and -dependent (53.4%) taxa. Site 3 was the only other location where estuarine-dependent taxa characterized greater than 20% of overall communities. Freshwater taxa accounted for ~2% or less of nekton communities across sites (Figure 7). Estuarine-resident dominated assemblages at Site 1 – 3 were attributed mostly to Grass Shrimp characterizing ~45 – 70% of nekton observed, whereas Bay Anchovy was the dominant taxa at Site 4 (79.8%). Bay Anchovy were also relatively abundant at Site 2 (22.8%). At Site 5, more even representation among guilds was due to dominance of Grass Shrimp (47.3%) and higher relative abundances of several estuarine-dependent taxa, such as Brown Shrimp (24.6%) and Blue Crab (8.9%). Relative abundance of estuarine-dependent taxa at Site 3 was low despite this guild being more diverse compared to most sites, which can be attributed to the accumulation of a greater number of taxa observed at lower densities, such as Blue Crab (9.8%), Estuarine Mud Crab (8.0%), and White Shrimp (4.9%) (Table 8).

Table 8. Summary of nekton counts, relative abundance (%), total counts, Shannon diversity, and taxa richness across five sites in the Guadalupe River Delta. Life history guilds are presented for each taxon and included freshwater (FW), estuarine-resident (ER), and estuarine-dependent (ED).

Family	Taxa	Guild	Site 1		Site 2		Site 3		Site 4		Site 5	
Mollusks			#	%	#	%	#	%	#	%	#	%
Mactridae	Atlantic Rangia	ER	4	0.06	5	0.07	2	0.08	0	0.00	3	0.30
Crustacean												
Cambaridae	Red Swamp Crayfish	FW	36	0.55	19	0.26	0	0.00	1	0.11	0	0.00
Palaemonidae	grass shrimp	ER	4324	66.57	3345	45.21	1516	60.25	5	0.55	470	47.33
Panopeidae	Estuarine Mudcrab	ED	2	0.03	24	0.32	201	7.99	0	0.00	15	1.51
Penaeidae	Brown Shrimp	ED	0	0.00	74	1.00	73	2.90	0	0.00	244	24.57
	Penaeidae sp.	ED	0	0.00	0	0.00	14	0.56	0	0.00	0	0.00
	White Shrimp	ED	1	0.02	108	1.46	123	4.89	15	1.66	29	2.92
Portunidae	Blue Crab	ED	41	0.63	94	1.27	246	9.78	4	0.44	88	8.86
-	larval shrimp	-	56	0.86	1	0.01	0	0.00	0	0.00	5	0.50
Fishes												
Achiridae	Hogchoker	ER	8	0.12	0	0.00	0	0.00	0	0.00	0	0.00
Atherinopsidae	Inland/Mississippi Silverside	ER	42	0.65	249	3.37	57	2.27	9	1.00	2	0.20
Centrarchidae	Bluegill	FW	30	0.46	0	0.00	0	0.00	1	0.11	0	0.00
	Florida/Largemouth Bass	FW	0	0.00	0	0.00	0	0.00	1	0.11	0	0.00
Characidae	Mexican Tetra	FW	15	0.23	1	0.01	0	0.00	0	0.00	0	0.00
Dorosomatidae	Gulf Menhaden	ED	688	10.59	176	2.38	27	1.07	92	10.18	26	2.62
	Skipjack Herring	ED	0	0.00	0	0.00	0	0.00	1	0.11	0	0.00
Cyprinodontidae	Sheepshead Minnow	ER	3	0.05	120	1.62	11	0.44	0	0.00	9	0.91
Elopidae	Ladyfish	ED	0	0.00	1	0.01	0	0.00	2	0.22	1	0.10
Engraulidae	Bay Anchovy	ER	70	1.08	1689	22.83	127	5.05	721	79.76	4	0.40
Fundulidae	Bayou Killifish	ER	19	0.29	98	1.32	1	0.04	0	0.00	1	0.10
	Bluefin Killifish	ER	60	0.92	4	0.05	0	0.00	0	0.00	0	0.00
	Golden Topminnow	ER	68	1.05	0	0.00	0	0.00	0	0.00	0	0.00
	Gulf Killifish	ER	12	0.18	38	0.51	9	0.36	0	0.00	3	0.30

Table 8 cont.

Family	Taxa	Guild	Site 1		Site 2		Site 3		Site 4		Site 5	
Fishes			#	%	#	%	#	%	#	%	#	%
Fundulidae	Rainwater Killifish	ER	7	0.11	4	0.05	1	0.04	0	0.00	0	0.00
Gerreidae	Flagfin Mojarra	ED	0	0.00	0	0.00	0	0.00	0	0.00	2	0.20
Gobiesocidae	Skilletfish	ED	0	0.00	0	0.00	3	0.12	0	0.00	0	0.00
Gobiidae	Code Goby	ER	5	0.08	8	0.11	17	0.68	0	0.00	15	1.51
	Highfin Goby	ER	0	0.00	0	0.00	3	0.12	0	0.00	1	0.10
	Naked Goby	ER	107	1.65	98	1.32	39	1.55	0	0.00	19	1.91
Ictaluridae	Channel Catfish	FW	1	0.02	0	0.00	0	0.00	1	0.11	0	0.00
Lepisosteidae	Longnose Gar	FW	1	0.02	0	0.00	0	0.00	1	0.11	0	0.00
Leuciscidae	Red Shiner	FW	0	0.00	0	0.00	0	0.00	1	0.11	0	0.00
Mugilidae	Striped Mullet	ED	0	0.00	2	0.03	4	0.16	8	0.88	2	0.20
Ophichthidae	Speckled Worm Eel	ED	0	0.00	0	0.00	3	0.12	0	0.00	0	0.00
Poeciliidae	Amazon Molly	ER	10	0.15	2	0.03	0	0.00	0	0.00	0	0.00
	Sailfin Molly	ER	297	4.57	827	11.18	0	0.00	4	0.44	0	0.00
	Western Mosquitofish	ER	527	8.11	371	5.01	4	0.16	37	4.09	1	0.10
Sciaenidae	Atlantic Croaker	ED	0	0.00	0	0.00	9	0.36	0	0.00	8	0.81
	Spot	ED	0	0.00	4	0.05	2	0.08	0	0.00	18	1.81
	Spotted Seatrout	ED	0	0.00	0	0.00	6	0.24	0	0.00	1	0.10
	Star Drum	ED	0	0.00	0	0.00	12	0.48	0	0.00	0	0.00
	Sheepshead	ED	0	0.00	23	0.31	1	0.04	0	0.00	26	2.62
Syngnathidae	Chain Pipefish	ER	21	0.32	1	0.01	0	0.00	0	0.00	0	0.00
		Taxa Richness	**44**		**31**		**29**		**17**		**24**	
		Shannon Diversity	**1.37**		**1.76**		**1.58**		**0.84**		**1.72**	
		Total	**6495**		**7398**		**2516**		**904**		**993**	

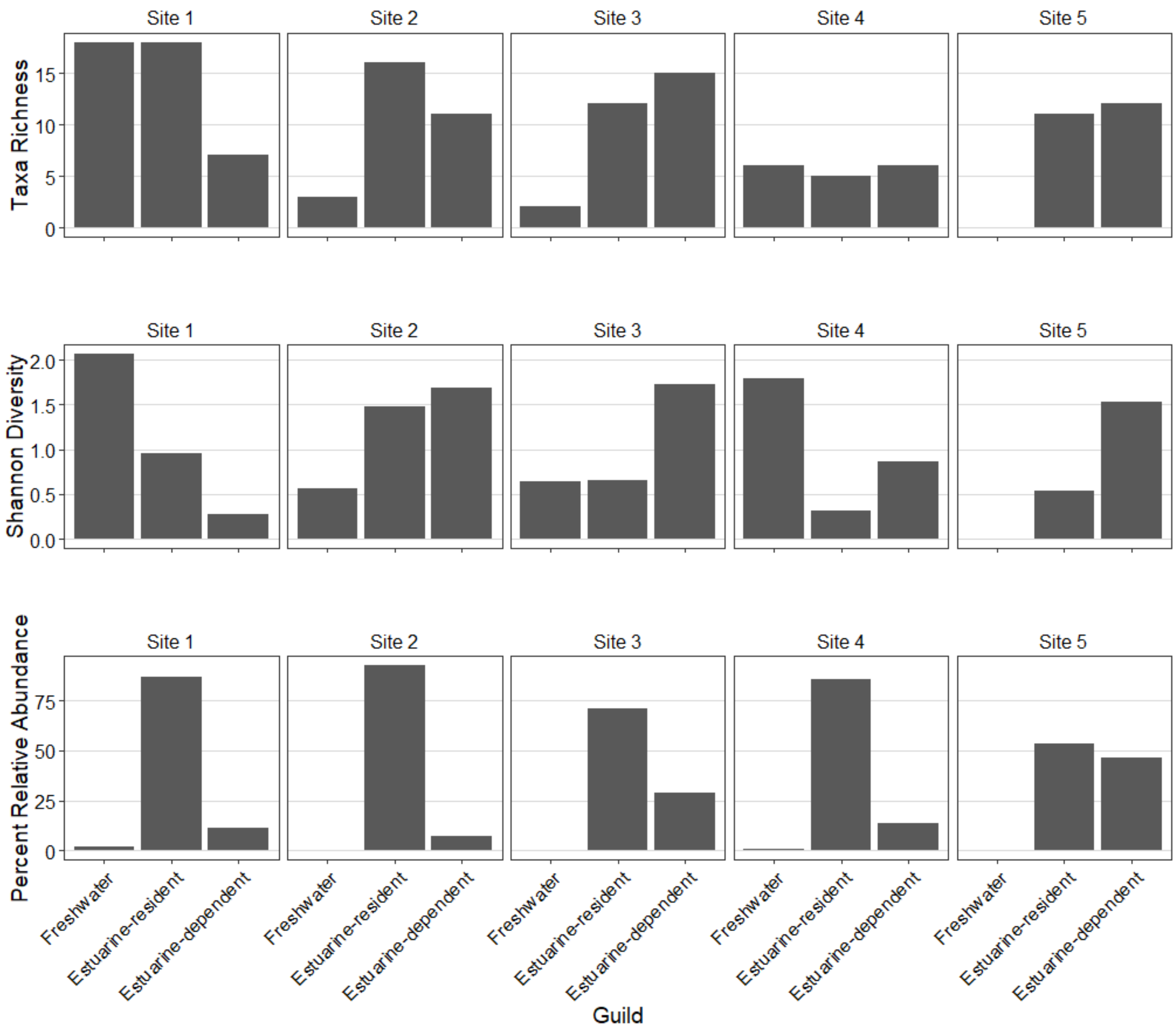

Figure 7. Bar graphs displaying site-level trends in taxa richness, Shannon diversity, and percent relative abundance of nekton among estuary usage guilds.

Relative abundance of estuarine-residents dominated nekton assemblages and accounted for ~75% of individuals at all sites except Site 5, which displayed more even relative abundances between estuarine-resident (46.6%) and -dependent (53.4%) taxa. Site 3 was the only other location where estuarine-dependent taxa characterized greater than 20% of overall communities. Freshwater taxa accounted for ~2% or less of nekton communities across sites (Figure 7). Estuarine-resident dominated assemblages at Site 1 – 3 were attributed mostly to Grass Shrimp characterizing ~45 – 70% of nekton observed, whereas Bay Anchovy was the dominant taxa at Site 4 (79.8%). Bay Anchovy were also relatively abundant at Site 2 (22.8%). At Site 5, more even representation among guilds was due to dominance of Grass Shrimp (47.3%) and higher relative abundances of several estuarine-dependent taxa, such as Brown Shrimp (24.6%) and

Blue Crab (8.9%). Relative abundance of estuarine-dependent taxa at Site 3 was low despite this guild being more diverse compared to most sites, which can be attributed to the accumulation of a greater number of taxa observed at lower densities, such as Blue Crab (9.8%), Estuarine Mud Crab (8.0%), and White Shrimp (4.9%) (Table 8).

Assemblage structure and habitat associations

The NMDS model converged after 50 runs fit using three dimensions and an ordination stress value of 0.17 indicated adequate model fit. A total of seven environmental vectors were considered strong predictors of site scores (i.e., $p < 0.05$) for the first two dimensions. Axis I mostly described a salinity ($r = 0.72$) gradient with low saline areas having higher prevalence of the freshwater-associated Water Hyacinth ($r = 0.46$). Axis II illustrated a gradient based on tide level ($r = 0.48$), water temperature ($r = 0.44$), and the mesohaline-associated Alkali Bulrush ($r = 0.38$). Lastly, vector coordinates for pH ($r = 0.36$) and Duckweed ($r = 0.30$) indicated these variables partially described both axes (Figure 8).

Visualization of site scores for the first two axes represent three general groupings of nekton communities. Axis I illustrated semi-discrete spatial shifts in assemblage structure associated with variation in salinity regimes across the delta. Specifically, axis I standard deviations for Site 1 and Site 4 did not overlap with Site 3 and Site 5, whereas Site 2 overlapped with all sites. Nekton assemblages at Site 1 and Site 4 were associated with lower salinities and Site 1 assemblages were associated with greater prevalence of Water Hyacinth. For example, species scores in close proximity to Site 1 scores included multiple freshwater taxa (e.g., Bluegill, Red Swamp Crayfish) and several estuarine-residents that are freshwater tolerant and associated with aquatic vegetation (e.g., Golden Topminnow, Bluefin Killifish, Chain Pipefish). At Site 3 and Site 5, assemblages were correlated with higher salinities, which aligned with species scores of estuarine-dependent taxa that are more associated with saline environments (e.g., Atlantic Croaker, Brown Shrimp, Blue Crab). Assemblage structure varied the most at Site 2, which was located near the center of the delta and had the most wide-ranging salinity regime. As such, species scores showing weak associations with axis I were taxa that can tolerate a wide breadth of salinity concentrations and predominantly included estuarine-resident fish (e.g., Naked Goby, Code Goby, Sheepshead Minnow) (Figure 8).

Axis II mostly described seasonal differences in assemblage structure. Among the two freshwater associated sites, Site 1 showed less variation along axis II compared to Site 4. Lower seasonal differences in assemblage structure at Site 1 can be best explained by most taxa associated with this site being estuary residents. In contrast, Ladyfish and Pinfish were associated with Site 4, which are estuarine-dependent species that utilize brackish environments during specific life history stages. Seasonal variation in Site 3 and Site 5 assemblages represent discrete time periods that estuarine-dependent taxa occupy estuaries. For example, Atlantic Croaker and Spot utilize estuaries during their spawning season in fall and winter, and these seasonal differences align with their species score's negative and positive associations with water temperature, respectively. Lastly, species scores of estuarine-dependent taxa showed minimal association with Site 2, which aligns with the weaker associations with water temperature displayed by this site (Figure 8).

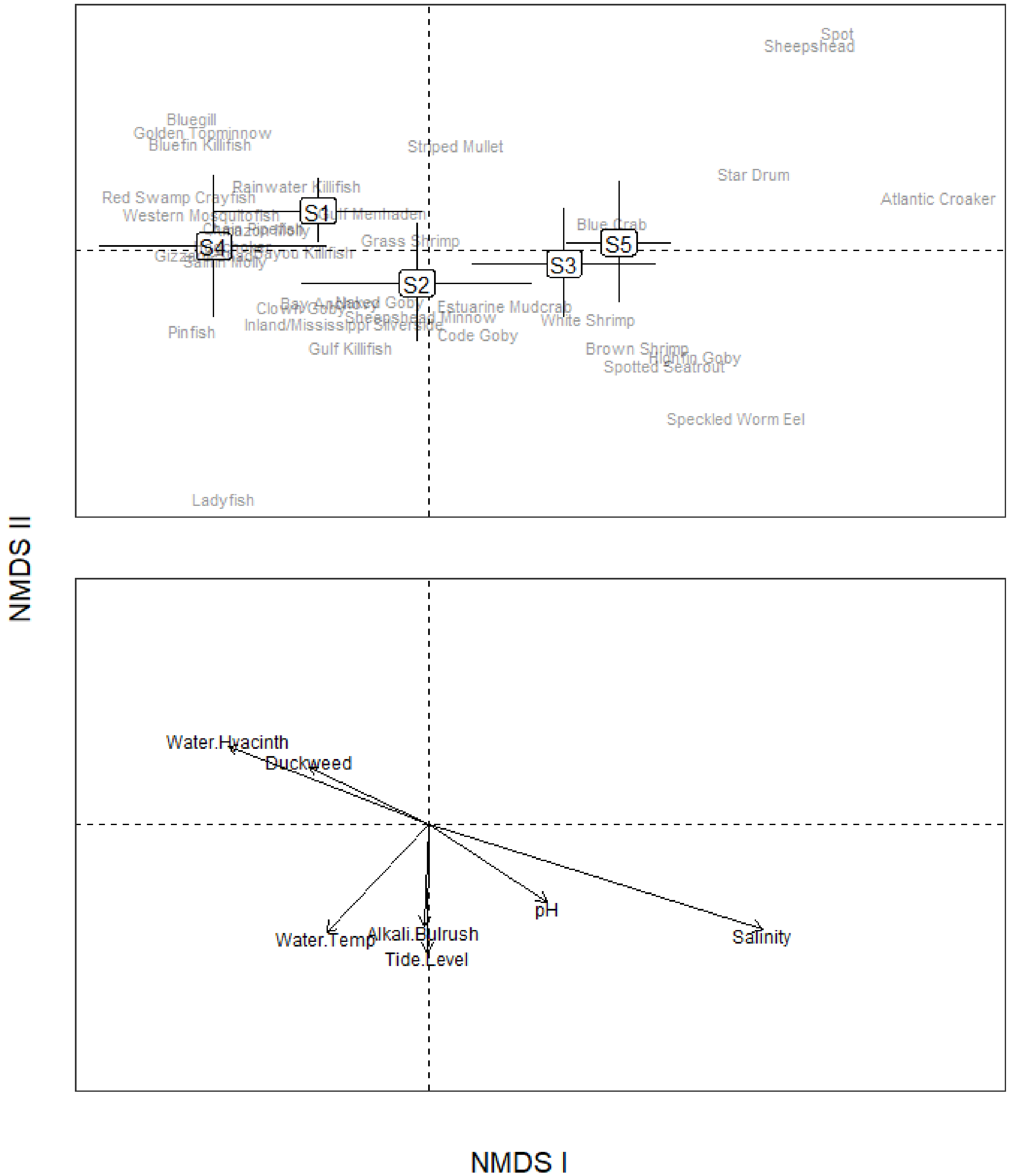

Figure 8. Two-dimensional nonmetric multidimensional scaling analysis displaying ordination of nekton assemblages and environmental vectors at five sites (S1-S5) in the Guadalupe River Delta. The top panel shows mean (± standard deviation) site scores and species scores and bottom panel denotes statistically significant ($p < 0.05$) environmental vectors that correlate with assemblage structure.

3.3.3 Effects of freshwater inflow and tidal regimes

Model selection procedures showed that the model with fixed effects, random effects, and dispersion sub-model with covariates was the best supported for data inference, which was consistently shown for all selection criteria. Specifically, delta AIC and BIC were 26 or more, AIC and BIC weights were close to one, and RMSE was about 2.5 times lower than the competing models (Table 9). The final model had a RMSE of 11.71 and residual standard deviation of 7.23, illustrating good predictive accuracy on average and within the random group-level predictors, respectively. In addition, conditional R^2 of 0.63 indicated both fixed and random effects predictors used to fit the model explained a relatively high proportion of variation in nekton density (Table 10).

Table 9. Comparisons of performance among competing models with alternate structure for predicting nekton density. Model performance for different combinations of fixed effects (FE), dispersion with covariates (D), and random effects (RE) sub-models were compared based on Akaike Information Criteria (AIC) and AIC weight, Bayesian Information Criteria (BIC) and BIC weight, and root mean squared error (RMSE).

Model	AIC (weight)	BIC (weight)	RMSE
FE	8761.47 (< 0.001)	8790.26 (< 0.001)	32.25
FE + D	8749.25 (< 0.001)	8789.56 (< 0.001)	32.39
FE + RE	7995.50 (< 0.001)	8041.56 (< 0.001)	27.08
FE + RE + D	7957.54 (> 0.999)	8015.12 (> 0.999)	11.71

Fixed effects terms represented average nekton community effects at the system-level. Mean nekton density was 0.41 (± 7.46) ind/m^2 based on the fixed intercept and when each covariate was at their average value. Both 90-day average tide level and 180-day high pulse frequency had a positive effect on nekton density and their coefficient's 95% confidence intervals did not overlap with zero. In addition, 90-day average tide level had a larger effect size and the best supported model included fitting this covariate with a quadratic term, meaning its effect was nonlinear (Table 10). Effect size of 90-day average tide level on density increased as 90-day tide level increased. From 0.46 to 0.60 m, nekton density estimates increased from about 3 to 6 ind/m^2 and further increased to a maximum density estimate of about 45 ind/m^2 as 90-day tide level increased to 0.73 m (Figure 9). Effect size of 180-day high flow frequency (0.05 ± 0.02) was lower than the linear term of 90-day average tide level (6.07± 2.04) (Table 10; Figure 9). As such, nekton density was estimated to increase from about 4 to 13 ind/m^2 as 180-day high flow pulse frequency increased from 2 to 26 days (Figure 9).

Despite the lower fixed intercept (i.e., average nekton density overall), random intercept variance was relatively high for the guild group-level predictor (Table 10). This indicated large differences in nekton density between estuary use guilds that weren't accounted for by the model's fixed terms. Large positive variance estimates for estuarine-resident crustaceans and fishes and estuarine-dependent crustaceans demonstrated mean density of these guilds were greater than the overall nekton community average. In contrast, larger negative variances for freshwater crustaceans and fishes showed they were less than the overall average. Estimate for estuarine-dependent fishes was slightly below the fixed intercept. Site-level random intercept variance was much lower relative to estuary use guild, meaning that spatial patterns of mean nekton density in the Delta didn't substantially differ from the system-level average (Table 10; Figure 10). Lastly, observation-level variance was also relatively high, suggesting local sampling or habitat factors within that were not accounted for may have had large effects on nekton density for multiple throw-trap samples (Table 10).

Under the quadratic parameterization for the dispersion sub-model, larger values of the dispersion parameter corresponded to a lower variance. The intercept was estimated to be 2.63 and vegetation coverage and salinity had a positive effect on the dispersion parameter, meaning that as each covariate increased, variance in nekton density decreased. Lastly, effect size on the dispersion parameter was larger for salinity (0.49 ± 0.28) relative to vegetation coverage (0.13 ± 0.10) (Table 10).

Table 10. Summary of parameter estimates with associated 95% confidence intervals (CI) and performance metrics for the final mixed effects model selected to predict nekton density.

	Estimate	**95% CI**
Fixed effects coefficients		
Intercept	-0.88	2.01
180-day high flow pulse frequency	0.05	0.02
90-day tide level (1)	6.07	2.04
90-day tide level (2)	25.81	17.42
Random effects standard deviation		
Estuary use guild	2.50	-
Site	0.15	-
Observation ID	1.98	-
Dispersion coefficients		
Intercept	2.63	2.12
Vegetation Cover	0.13	0.10
Salinity	0.49	0.28
Predictive Performance		
Conditional R^2	0.63	-
Root mean squared error	11.71	-
Residual standard deviation	7.23	-

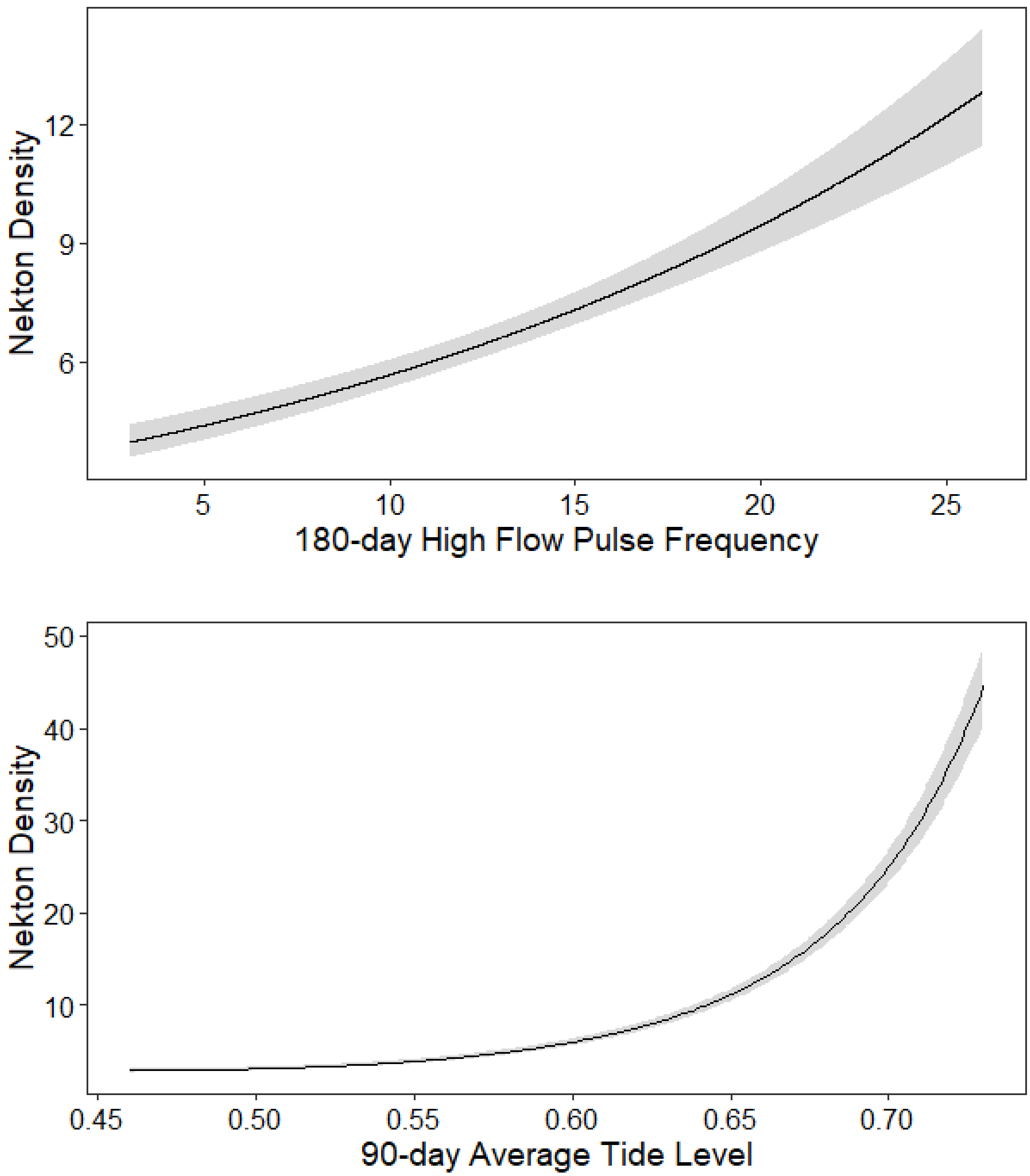

Figure 9. Fixed effects model predictions of nekton density (individuals/m^2) as a function of 90-day high flow pulse frequency (days) and 90-day average tide level (m) at the Guadalupe River Delta. Solid lines represent line-of-best-fit and grey polygons denote 95% confidence intervals.

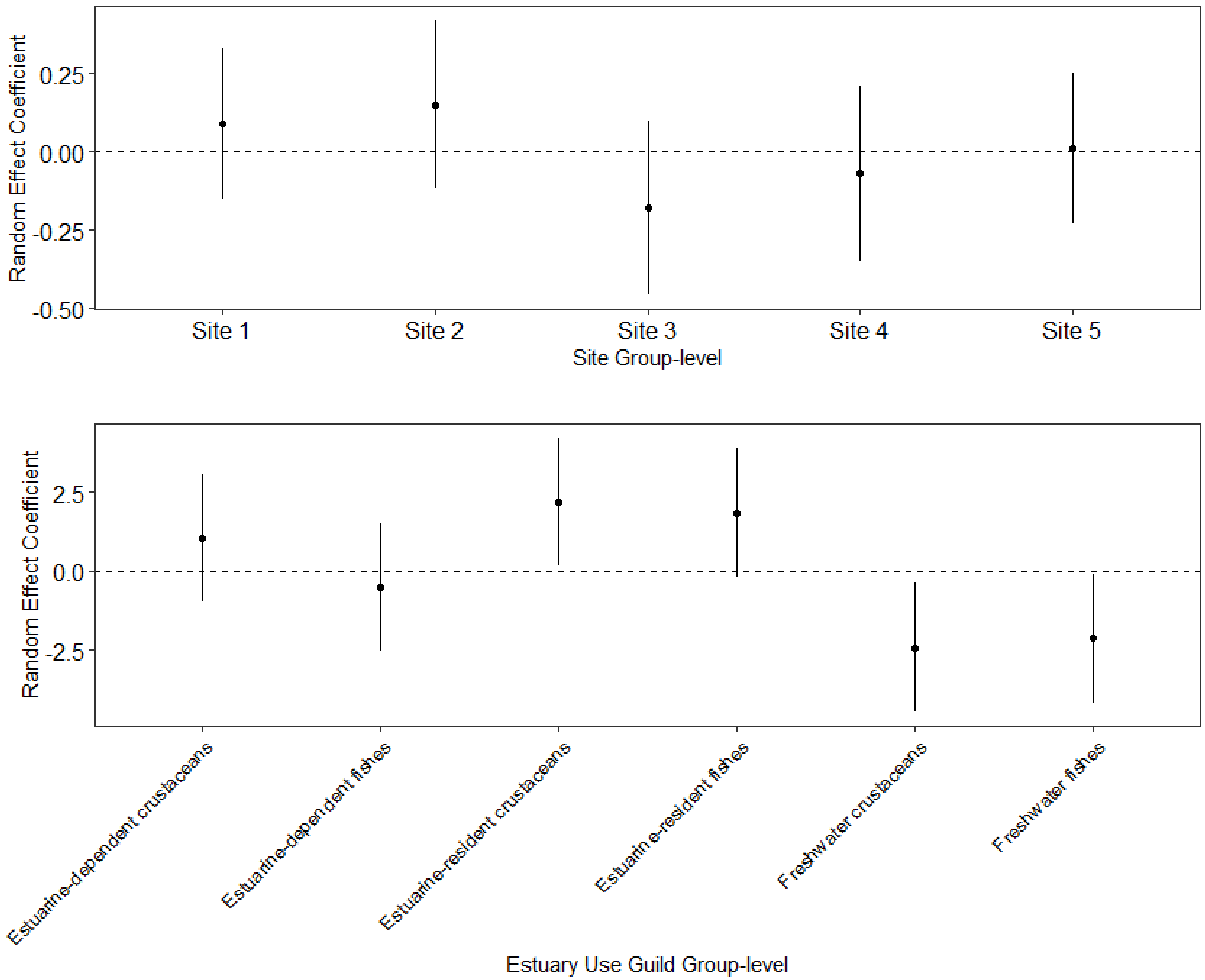

Figure 10. Random coefficient estimates (± 95% confidence intervals) among site and estuary use guild group-levels for predicting nekton density. Coefficients close to zero illustrate group-levels with estimates more similar to the fixed effect intercept estimate (i.e., average nekton community effects at the system-level).

4.0 DISCUSSION

4.1 Vegetation and Avian Communities

Vegetation community compositions observed in 2023 were generally similar to past surveys at Site 1-3. Dominance was captured differently between 2019, 2021, and 2023 sampling, including both new dominant species and previously unreported species. Differences in dominance may be a function of heterogeneity in sampling methodology and the increased vegetative sampling effort. Conversely, this may also suggest that marsh vegetation communities within the Delta fluctuate largely on both an inter-seasonal and inter-annual basis. Regardless of the mechanism, results demonstrated vegetation communities show local temporal and spatial shifts in composition within sites and support the presence of a longitudinal gradient of species composition. Spatial patterns of vegetation communities reflected long-term salinity regimes across the Delta, transitioning from more freshwater-associated assemblages near freshwater inflow sources to euryhaline marsh assemblages in areas closer to marine influences.

Despite within-site differences in vegetation species dominance, Site 1 remained a predominantly herbaceous aquatic species assemblage, whereas graminoid marsh species were most characteristic of assemblages at Site 2-3. Site 4 illustrated the most diverse vegetation assemblages that contained graminoid, herbaceous, and shrub species documented at other sites, as well as several unique species (e.g., Spider Lily, Swamp Lily). Vegetation assemblages at Site 5 differed from other sites in close proximity to bays. This can mainly be attributed to the spatial extent of this site including riparian habitats along Towsend Bayou, which contained multiple shrub species. Carolina Wolfberry, a notable food source for the Whooping Crane, was also documented at Site 5 during both seasons.

Avian community sampling was added to the 2021 and 2023-2024 data collection efforts and provided a baseline for the assessment of future fluctuations in avian abundance, diversity, and habitat associations in the Delta. The avian diversity and presence of two federally-listed species (i.e., Eastern Black Rail, Whooping Crane) within marsh habitat indicates how important these areas are to sustaining robust communities. The salinity gradient and resulting heterogeneity in vegetation and faunal community compositions likely affect avian abundance and drive avian distribution within the Delta (Armitrage et al 2007; VanDusen 2012).

Eastern Black Rail was observed during 2021 surveys, but not detected in 2023 or 2024. That said, it is plausible that the species was present but not detected while surveying. Eastern Black Rail is considered cryptic due to their utilization of densely vegetated marsh habitats, as well as infrequent flying and vocalization behavior (Eddleman et al. 1988; Sibley 2000). Adding new species-specific sampling techniques with the current point count methodology may help increase Eastern Black Rail detectability in the future. Whooping Crane, in contrast, was not detected in 2021, but was observed at Site 5 in 2024. This can be attributed to the addition of winter bird surveys when the species utilizes estuarine habitats along the Texas Gulf Coast (Sibley 2000). Whooping Crane utilization of habitats at Site 5 may have been linked to the presence of Carolina Wolfberry at this site (Chavez Ramirez 1996). Lastly, neither species were detected by automated recorders, suggesting the need to select additional or alternate deployment locations in the future.

4.2 Nekton Community

Results from throw-trap sampling supported observations from previous assessments associated with this study, while also providing new insights into potential mechanisms that drive nekton community patterns. Variation in environmental conditions across sites and taxa richness, diversity, and relative abundance across estuary use guilds in the Guadalupe Delta aligned with expectations (BIO-WEST 2020, 2022). Similar to other Texas coastal marsh systems, estuarine-residents were typically the most diverse and abundant guild throughout the Delta, whereas freshwater taxa were the least abundant, but were more diverse at sites closer to freshwater inflow sources (i.e., tidal freshwater habitats). Estuarine-dependents were most associated with areas directly connected to bays that experience greater interactions with marine environments (Longley 1994; Ley et al. 1999; Akin et al. 2003). Trends in nekton assemblages further support that differences in dynamic habitat components best explain spatial structure, with magnitude of dissimilarities depending on relative distances from freshwater inflow and bays, as well as salinity regimes (Peterson 2003). Lastly, freshwater inflow and tidal regimes affected variation in nekton density, with tide level effects illustrating a nonlinear relationship, emphasizing that the Guadalupe River Delta is a complex and dynamic estuarine system (Methven et al. 2001; Elliot and Hemingway 2002; Montagna et al. 2011).

Spatiotemporal variation in nekton assemblage structure was explained by both stationary and dynamic habitat components. Spatial dissimilarities in structure between the three general assemblage groupings were mostly explained by differences in salinity regimes across the river delta, supporting that salinity is a focal driver on the spatial organization of nekton communities (Akin et al. 2003; Montagna et al. 2011; Montagna et al. 2013). Site 1 and 4 were distinct from other sites because they provided habitat for a diversity of freshwater taxa (e.g., Red Swamp Crayfish, centrarchid fishes) and resident taxa tolerant of a wide range of salinities (e.g., Bay Anchovy, poecilid fishes). Moreover, Site 1 assemblages differed from all other sites due to the consistent availability of Water Hyacinth along marsh edges, providing suitable habitat for taxa associated with macrophytes and tolerant of low saline conditions (e.g., fundulid fishes) (Rozas and Minello 1997; Castellanos and Rozas 2001). At Site 2, there are several factors that potentially explain its intermediary structuring. Site 2 experienced more frequent high salinity conditions compared to Site1 and 4 and vegetation cover was more frequently available along the marsh edge compared to Site 3 and 5. As such, assemblages at Site 2 harbored taxa tolerant of wide ranges in salinity and associated with marsh vegetation that were common at other sites (e.g., Inland/Mississippi Silverside, Bay Anchovy, Code Goby, Grass Shrimp). Site 2 assemblages were also more frequently dominated by grass shrimp.

Dissimilarities of assemblages at Site 3 and 5 were due to greater richness and diversity of estuarine-dependent taxa (e.g., Brown Shrimp, Blue Crab), indicating that areas directly connected to adjacent bays systems provide important habitat for marine migrants that utilize the Delta during particular life history stages (Secor and Rooker 2005; Rozas et al. 2013). That said, two estuarine-dependent fishes (i.e., Ladyfish, Pinfish) were more associated with tidal freshwater habitats at Site 4. Ladyfish and Pinfish are relatively active and mobile species, and therefore, utilize a greater diversity of habitats (Adams et al. 2013; Faletti et al. 2019). Water temperature provided a partial explanation for the observed within-site temporal dissimilarities in nekton assemblages, particularly at Site 3 and 5 that harbored a greater density of marine migrants. This may be related to seasonality in life history cycles for estuarine dependent taxa.

For example, Ladyfish were associated with warmer waters and are known to utilize estuaries in the fall, whereas Spot were associated with cooler temperatures and known to utilize estuaries in the winter (Warlen and Chester 1985; McBride and Horodysky 2004). Further, associations of Blue Crab, White Shrimp, and Brown Shrimp with water temperature were not as strong compared to other estuarine-dependent taxa, due to their use of estuaries being relative to ontogenetic stage (Zein-Eldin and Renaud 1986; Riera et al. 2000; Kennedy et al. 2007). For example, Brown Shrimp post-larvae immigrate into estuaries from winter to early spring and emigrate back into bays as juveniles from late spring to summer (Riera et al. 2000). As mentioned previously, temporal variation within sites was also partially explained by tide-level which could have an effect on the availability of vegetation cover along the marsh edge, especially within sites closer to bays (BIO-WEST 2022).

The mixed effects model used to estimate nekton density proved to be useful for assessing how system-level processes and local habitat conditions may influence patterns in biological productivity. Model results suggested 180-day high pulse frequency had a positive effect on nekton density as it increased to 26 days. This relationship supports the general notion that increased freshwater inflows have a positive effect on estuary function. More frequent high flows potentially result in greater inputs of material and energy (e.g., organics, sediment), thus stimulated biological productivity (Montagna et al. 2011; Montagna et al. 2025). Positive effects of high flow pulses would be expected to attenuate as its frequency increases and manifests more uniform low saline conditions, though given the flow regimes observed during this study, the change point where this might occur is currently unknown (Montagna and Kalke 1992; Peterson 2003; Quigg et al. 2009; Montagna et al. 2011). Similarly, nekton densities were predicted to be lowest when high flow pulse frequency was near zero, which was associated with increased salinities that potentially reduced the abundance of some estuarine-resident and freshwater taxa less tolerant to high saline conditions (Longley 1994; Beseres-Pollack et al. 2011; Palmer et al. 2011).

Effect size of 90-day average tide level on nekton density depended on the given value across its range, illustrating a complex nonlinear functional response by nekton to recent tidal regime characteristics. Compared to freshwater inflow, 90-day average tide level had a greater influence on changes in nekton density, supporting that tide patterns also play an important role in estuary function. Positive associations of nekton abundance with higher tide levels have been documented by previous studies, which have suggested this relationship primarily manifests due to increased availability and connectivity of vegetated edge habitats (Roman et al. 2002; Roth et al. 2008; de la Barra et al. 2022). Past research has shown water exchanged by tidal flooding not only increases edge habitat availability and connectivity throughout an estuary, but also transports material and energy, which may explain why estimated nekton density was greatest at the highest 90-day average of 0.73 m (Sheaves and Johnston 2008; Montagna et al. 2011; Hyndes et al. 2014). This is further supported by the sharp nonlinear increase in effect size as average tide-level rose above 0.6 m. Like other estuaries in the Gulf of Mexico, the Guadalupe Estuary has a smaller tide range at a maximum of about 1 m, though is the only closed bay system that lacks a direct connection to the Gulf of Mexico due to Matagorda Island acting as a barrier (Opdyke et al. 2025). Based on this in total, it is possible that in addition to increased areas of inundation, transportation and exchange of material and energy is limited when tide interactions are lower, but start to increase substantially past a certain threshold, resulting in a large spike in biological productivity. Elevated tide levels were also likely conducive to more frequent higher saline conditions for a diverse array of euryhaline nekton taxa and may also provide some explanation for the estimated trends by the model (Akin et al. 2003; Montagna et al. 2011). Lastly, the dispersion sub-model suggested nekton densities were spatially heterogeneous on average and became less clustered when salinity and vegetation cover was higher. This provides evidence to suggest biological productivity is relatively more homogenous throughout areas that exhibit more saline conditions and with a greater availability of vegetation cover. As such, tide level during discrete periods in time should play a large role in the spatial organization of nekton density, since it influences both salinity concentration and vegetation available along marsh edges, particularly in areas adjacent to bays.

5.0 CONCLUSION

In summary, the vegetation communities sampled in 2023 exhibited a gradient of freshwater-associated to saltwater-associated species assemblages similar to that reported in previous years. Areas closer to the freshwater influence of the Guadalupe River were characterized by emergent freshwater marsh plants and non-native species, while sites further from freshwater inflow sources and closer to tidal influence were generally dominated by facultative halophytes. The expanded spatial scope of this study since 2021 likely contributed to the increased vegetative species overlap and diversity observed among Site 1-3. The addition of two new sites also provided a greater understanding on spatial patterns in vegetation communities across the Delta. Most significantly, the prevalence of Carolina Wolfberry at Site 5 indicated emergent marshes in this area provide food resources and habitat for the endangered Whooping Crane.

The avian community assessment demonstrated the high-level of diversity present within the Delta. This estuary provides a wide array of habitat types which support migratory and resident species from a variety of foraging guilds. Inclusion of Site 4 and 5 and a winter survey event helped to better characterize both the spatial and temporal variability of avian assemblage structure throughout the Delta and resulted in positive detections of Whooping Crane. Surveys failed to detect Eastern Black Rail, though recent observations of this cryptic species during 2021 surveys suggest it likely still occurs in the Delta. Species-specific survey techniques could potentially improve detectability of Eastern Black Rail and help to better understand their population. Lastly, neither species were detected by automated recorders, suggesting the need to select alternate and/or additional deployment locations in the future.

Assessments of nekton communities over the entire study duration both supported results from previous analyses and provided new insights to help better understand potential mechanisms driving spatiotemporal trends in nekton assemblages and biological productivity in the Delta. Spatiotemporal variation in nekton assemblage structure and among estuary use guilds were associated with both functionally stationary (e.g., vegetation) and dynamic (e.g., salinity) habitat components (Peterson 2003). Most significantly, the mixed effects model used for this report was able use freshwater inflow and tide characteristics to predict variation in nekton density with good accuracy. Results from the final model selected for inference indicated effects of 180-day high flow pulse frequency were linear, whereas effects of 90-day average tide level were nonlinear, further supporting that interactions between large scale environmental processes and biotic communities in estuaries are complex (Methven et al. 2001; Elliot and Hemingway 2002; Montagna et al. 2013). The positive effect illustrated by 180-day high flow pulse frequency on nekton density demonstrated that increases in freshwater inflow can enhance biological productivity (Peterson 2003; Montagna et al. 2011; Montagna et al. 2025). In addition to freshwater inflow, the stronger relationship illustrated between tide level and nekton density suggests maintaining hydrologic connectivity between the Delta and bay complexes is also important (Roman et al. 2002; Roth et al. 2008; de la Barra et al. 2022). In total, this supports freshwater inflow and tidal regimes are both key determinants of biological productivity in the upper Guadalupe Estuary.

6.0 LITERATURE CITED

Adams, A.J., A.Z. Horodysky, R.S. McBride, K. Guindon, J. Shenker, T.C. MacDonald, H.D. Harwell, R. Ward, K. Carpenter. 2013. Global conservation status and research needs for tarpons (Megalopidae), ladyfishes (Elopidae) and bonefishes (Albulidae). Fish and Fisheries 15:280-311.

Akin, S., K. O. Winemiller, and F. P. Gelwick. 2003. Seasonal and spatial variations in fish and macrocrustacean assemblage structure in Mad Island Marsh Estuary, Texas. Estuarine, Coastal, and Shelf Science. 57:269-282.

Alber, M. 2002. A conceptual model of estuarine freshwater inflow management. Estuaries. 25:1246-1261.

Armitrage, A. R., S. M. Jensen, and R. F. Ambrose. 2007. Wintering shorebird assemblages and behavior in restored wetlands in Southern California. Restoration Ecology. 15:139-148.

Basin and Bay Expert Science Team (BBEST). 2011. Environmental Flows Recommendations Report: Final Submission to the Guadalupe, San Antonio, Mission, and Aransas Rivers and Mission, Copano, Aransas, and San Antonio Bays Basin and Bay Area Stakeholder Committee, Environmental Flows Advisory Group, and Texas Commission on Environmental Quality. Austin, Texas.

Beseres-Pollack, J., T.A. Palmer, and P.A. Montagna. 2011. Long-term trends in the response of benthic macrofauna to climate variability in the Lavaca-Colorado Estuary, Texas. Marine Ecology Progress Series 436:67-80.

Bio-West, Inc. (BIO-WEST). 2020. Seasonal ecological assessment in the upper Guadalupe estuary. Technical Report. Prepared for Guadalupe-Blanco River Authority.

Bio-West, Inc. (BIO-WEST). 2022. Seasonal ecological assessment in the upper Guadalupe estuary. Technical Report. Prepared for Guadalupe-Blanco River Authority.

Brooks, M. 2024. glmmTMB: Generalized linear mixed effects models using template model builder. R package version 1.1.9.

Burdick, D. M., and Konisky, R. A. 2003. Determinants of expansion for *Phragmites australis*, common reed, in natural and impacted coastal marshes. Estuaries. 26: 407-416.

Castellanos, D.L., and L.P Rozas. 2001. Nekton use of submerged aquatic vegetation, marsh, and shallow unvegetated bottom in the Atchafalaya River delta, a Louisiana tidal freshwater ecosystem. Estuaries 24:184-197.

Chamberlain, S. rnoaa: R interface to many NOAA data sources. R package version 1.4.0.

Cowan, J.H., A. Yanez-Arancibia, P. Sanchez-Gill, and L.A. Deegan. 2013. Estuarine Nekton. Pages 327-357 *in* Estuarine Ecology, Second Edition. Wiley-Blackwell, Hoboken, NJ.

Day, J. W., Jr., C. A. S. Hall; W. M. Kemp, and A. Yanez-Arancibia. 1989. Estuarine Ecology. John Wiley and Sons, New York, NY.

DeCicco, L. 2022. dataRetrieval: Retrieval function for USGS and EPA hydrologic and water quality data. R package version 2.7.11.

de la Barra, P., M. Skov, P. Lawrence, J.I. Schiaffi, and J.G. Hiddink. 2022. Tidal water exchange drives fish and crustacean abundances in salt marshes. Marine Ecology Progress Series 694:61-72.

Eddleman, W. R., F. L. Knopf, B. Meanly, F. A. Reid, and R. Zembal. 1988. Conservation of North American rallids. Wilson Bulletin 100:458-475.

Elliot, M., and K. L. Hemingway, editors. 2002. Fishes in Estuaries. Blackwell Science Ltd, Oxford, UK.

Faletti, M.E., D.H. Chacin, J.A. Peake, T.C. MacDonald, and C.D. Stallings. 2019. Population dynamics of Pinfish in the eastern Gulf of Mexico (1998-2016). PLoS ONE 14: e0221131. https:// doi.org/10.1371/journal.pone.0221131.

Goberville, E., G. Beaugrand, B. Sautour, and P. Treguer. 2011. Evaluation of coastal perturbations: a new mathematical procedure to detect changes in the reference state of coastal systems. Ecological Indicators. 11:1290-1300.

Harrison, X.A. 2014. Using observation-level random effects to model overdispersion in count data in ecology and evolution. PeerJ 2:e616.

Hyndes, G.A., I. Nagelkerken, R.J. McLeod, R.M. Connolly, P.S. Lavery, and M.A. Vanderklift. 2014. Mechanisms and ecological role of carbon transfer within coastal seascapes. Biological Reviews 89:232-254.

Jordan, F., S. Coyne, and J. C. Trexler. 1997. Sampling fishes in vegetated habitats: Effects of habitat structure on sampling characteristics of the 1-m^2 throw trap. Transactions of the American Fisheries Society. 126:1012-1020.

Kennedy, V.S., and L.E. Cronin, editors. 2007. The Blue Crab *Callinectes sapidus*. Maryland Sea Grant College, College Park, MD.

Ley, J. A., C. C. McIvor, and C. L. Montague. 1999. Fishes in mangrove prop-root habitats of northeastern Florida Bay: distinct assemblages across an estuarine gradient. Estuarine, Coastal, and Shelf Science 48:701-723.

Linden, A., and S. Mantyniemi. 2011. Using negative binomial distribution to model overdispersion in ecological count data. Ecology 92:1414-1421.

Loneragan, N. R., I. C. Potter, and R. C. J. Lenanton. 1989. Influence of site, season, and year on contributions made by marine estuarine, diadromous, and freshwater species to the fish fauna of a temperate Australian estuary. Marine Biology. 103:575-586.

Longley, W. L., editor. 1994. Freshwater inflows to Texas bays and estuaries: ecological relationships and methods for determination of needs. Texas Water Development Board and Texas Parks and Wildlife Department, Austin, TX.

Lüdecke, D. 2024a. performance: Test if your model is a good model. R package version 0.12.1

Lüdecke, D. 2024b. parameters: Describe and understand your model's parameters. R package version 0.22.0.

Lüdecke, D. 2024c. ggeffects: estimated marginal means and adjusted predictions for regression models. R package version 1.1.3.

Makowski, D. 2024. modelbased: Taking your models to new heights. R package version 0.8.7.

Matagorda Bay Health Evaluation (MBHE). 2007. Final Report: Matagorda Bay Health Evaluation Habitat Assessment. Prepared for Lower Colorado River Authority and San Antonio Water Systems. June 2007.

McBride, R.S., and A.Z. Horodysky. 2004. Mechanisms maintain sympatric distributions of two ladyfish (Elopidae: Elops) morphs in the Gulf of Mexico and western North Atlantic Ocean. Limnology and Oceanography 49:1173-1181.

McGarigal, K., S. Stafford, and S. Cushman. 2000. Multivariate Statistics for Wildlife and Ecology Research. Springer, New York, NY.

Methven, D. A., R. L. Haedrich, and G. A. Rose. 2001. The fish assemblage of a Newfoundland estuary: Diel, monthly, and annual variation. Estuarine, Coastal, and Shelf Science 52:669-687.

Montagna, P.A., and R.D. Kalke. 1992. The effect of freshwater inflow on meiofaunal and macrofaunal populations in the Guadalupe and Nueces estuaries. Estuaries 15:307-326.

Montagna, P. A., B. Vaughan, and G. Ward. 2011. The Importance of Freshwater Inflows to Texas Estuaries. Pages 107-127 *in* Water Policy in Texas: Responding to the Rise of Scarcity. Taylor & Francis, New York, NY.

Montagna, P. A., T. A. Palmer, and J. B. Pollack. 2013. Conceptual Model of Estuary Ecosystems. Pages 5-21 *in* Hydrological Changes and Estuarine Dynamics. Springer, New York, NY.

Montagna, P. A., R.D. Kalke, and L.J. Hyde. 2025. Effect of Freshwater Inflow on Benthic Infauna. Pages 259-294 *in* Freshwater Inflows to Texas Bays and Estuaries: A Regional-scale Review, Synthesis, and Recommendations. Springer, Chams, Switzerland.

Morton, R. A., and A.C. Donaldson. 1978. Hydrology, morphology, and sedimentology of the Guadalupe fluvial-deltaic system. Geological Society of America Bulletin. 89:1030-1036.

Oksanen, J. 2022. vegan: Community Ecology Package. R package version 2.6.2.

Opdyke, D., J. Hoffmann, P.A. Montagna, and J.F. Trungale. 2025. Hydrology, Circulation, and Salinity. Pages 85-142 *in* Freshwater Inflows to Texas Bays and Estuaries: A Regional-scale Review, Synthesis, and Recommendations. Springer, Chams, Switzerland.

Palmer, T. A., P. A. Montagna, J. B. Pollack, R. D. Kalke, and H. R. DeYoe. 2011. The role of freshwater inflow in lagoons, river, and bays. Hydrobiologia. 667:49-67.

Peterson, M.S. 2003. A conceptual view of environment-habitat-production linkages in tidal river estuaries. Reviews in Fisheries Science 11:291-313.

Quigg, A., L. Broach, W. Denton, and R. Miranda. 2009. Water quality in the Dickinson Bayou watershed (Texas, Gulf of Mexico) and health issues. Marine Pollution Bulletin. 58:896-904.

Riera, P., P.A. Montagna, R.D. Kalke, and P. Richard. 2000. Utilization of estuarine organic matter during growth and migration by juvenile brown shrimp *Penaeus aztecus* in a South Texas estuary. Marine Ecology Progress Series 199:205-216.

Roman, C.T., K.B. Raposa, S.C. Adamowicz, M.J. James-Pirri, and J.G. Catena. 2002. Quantifying vegetation and nekton response to tidal restoration of a New England salt marsh. Restoration Ecology 10:450-460.

Roth, B.M., K.A. Rose, L.P. Rozas, and T.J. Minello. 2008. Relative influence of habitat fragmentation and inundation on brown shrimp *Farfantepenaeus aztecus* production in northern Gulf of Mexico salt marshes. Marine Ecology Progress Series 359:185-202.

Rozas, L. P., and T. J. Minello. 1997. Estimating densities of small fishes and decapod crustaceans in shallow estuarine habitats: A review of sampling design with focus on gear selection. Estuaries 20:199-213.

Rozas, L.P., C.W. Martin, and J.F. Valentine. 2013. Effects of reduced hydrological connectivity on nursery use of shallow estuarine habitats within a river delta. Marine Ecology Press Series 492:9-20.

Secor, D.H., and J.R. Rooker. 2005. Connectivity in the life histories of fishes that use estuaries. Estuarine Coastal and Shel Science 64:1-3.

Shannon, C.E. 1948. A mathematical theory of communication. The Bell System Technical Journal. 27: 379-423.

Sheaves, M., and R. Johnston. 2008. Influence of marine and freshwater connectivity on the dynamics of subtropical estuarine wetland fish metapopulations. Marine Ecology Progress Series 357:225-243.

Sibley, D. A. 2000. The Sibley guide to birds, first edition. Knopf, New York, NY.

Steichen, J. L., and A. Quigg. 2018. Fish species as indicators of freshwater inflow within a subtropical estuary in the Gulf of Mexico. Ecological Indicators. 85:180-189.

Stunz, G. W., J. C. Gibeaut, E. L. Oborny, P. T. Plotkin, J. B. Pollack, J. R. Rooker, R. J. D. Wells, and M. S. Wetz. 2023. Matagorda Bay Ecosystem Assessment Technical Report. Texas Comptroller of Public Accounts CMD 19-6799CS.

Stutzenbaker, C. D. 1999. Aquatic and Wetland Plants of the Western Gulf Coast. Texas Parks and Wildlife Press, Austin, TX.

United States Department of Agriculture (USDA), Forest Service. 1997. Monitoring bird populations by point counts. General technical Report. PSW-GTR-149.

United States Department of Agriculture (USDA) Natural Resources Conservation Service (NRCS). 2000. Plant guide to smooth cordgrass. https://plants.usda.gov/plantguide/pdf/pg_spal.pdf

VanDusen, B. M., S. R. Fegley, and C. H. Peterson. 2012. Prey distribution, physical habitat features, and guild traits interact to produce contrasting shorebird assemblages among foraging patches. PLoS One. 7:e52694.

Verner, J. 1985. Assessment of counting techniques. Current Ornithology. 2:247-302.

Warlen, S.M., and A.J. Chester. 1985. Age, growth, and distribution of larval spot, *Leiostomus xanthurus*, off North Carolina. U.S. National Marine Service Fishery Bulletin 83:587-599.

Zein-Eldin, Z.P., and M.L. Renaud. 1986. Inshore environmental effects of Brown Shrimp, *Penaeus aztecus*, and White Shrimp, *P. setiferus*, populations in coastal waters, particularly of Texas. Marine Fisheries Review 48:9-19.